AN ABSTRACT OF THE THESIS OF

Akbar Khurshid for the degree of Master of Science in Geology presented on January 24, 1991.

Title: Crustal Structure of the Sulaiman Range, Pakistan, From Gravity Data.

Abstract approved: Robert J Lillie

Robert J. Lillie

Gravity data along an east-west profile from the Punjab plain of Pakistan to the western border town of Chaman have been incorporated into interpretation of the gross crustal structure underlying the Sulaiman Range. Interpretation of the free-air, Bouguer, and isostatic gravity anomalies suggests that 15 to 25 km thick, transitional crust underlies the 250 km wide fold-and-thrust belt. Thick overlying sediments are compensated by shallow mantle material, which leads to a long wavelength (~200 km) Bouguer gravity high in the area. Free-air and isostatic anomalies suggest that high topography in the eastern Sulaiman Range lacks roots, as the Moho apparently shallows beneath the thick (>15 km) sediments. In the western Sulaiman Range the topography appears to be compensated by thicker crust.

Interpretation of transitional crust in the region suggests that passive margin structures identified along the western edge of the Indo-Pakistani subcontinent continue under the Sulaiman foldbelt, and that the region is at an early stage of continental collision. The crust appears to be deformed under the load of the thrust belt and the influence of horizontal compressive forces resulting from the convergence of the Indian subcontinent against the Afghan Block. Crustal thickening is taking place on the west, as the Indo-Pakistani plate is underthrusting continental crust of this block.

Crustal Structure of the Sulaiman Range, Pakistan, From Gravity Data

by

Akbar Khurshid

A THESIS
submitted to
Oregon State University

in partial fulfillment of
the requirements for the
degree of

Master of Science

Completed January 24, 1991
Commencement June, 1991

APPROVAL:

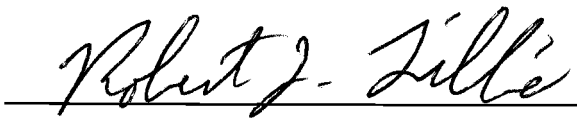

Associate Professor of Geology and Geophysics in charge of major

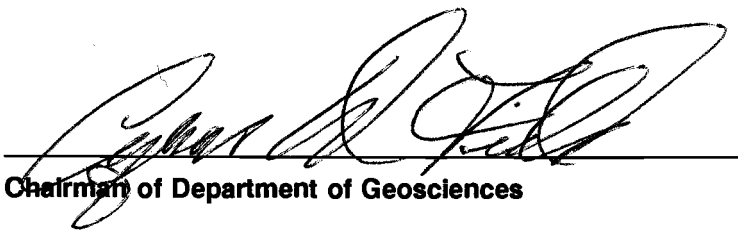

Chairman of Department of Geosciences

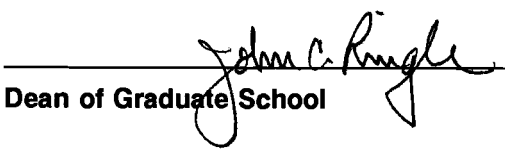

Dean of Graduate School

Date thesis is presented January 24, 1991

Student Name Akbar Khurshid

ACKNOWLEDGEMENTS

My foremost thanks to Bob Lillie for accepting me as his student and offering an opportunity to work on a project of my own country. Many thanks for his dynamic, sharp and critical guidance, which ultimately made me think independently and write with confidence. I also had a good time with him as a friend and always felt free talking to him without any formal appointment.

This work has benefited from the kindness, cooperation, and fruitful discussion with Bob Lawrence, which improved the realization of this thesis. My thanks to my senior colleague Russell Nazirullah for conducting the gravity traverses in the rugged Sulaiman region, which provided the fundamental data for this research work.

I take this moment to thank all my Pakistani and non-Pakistani friends, particularly Kausar, Mansoor, Baig, Jadoon, Mazhar, Irshad, Soofi, Daniel, Li, and Jochen. Many thanks to all of you for all that you people have done for me.

Many thanks to my beloved wife Mahreen for her patience, support and true friendship since 1978. Thanks to my family members, particularly Javed, my brother Qamar and sisters for their warm emotional support.

Finally, I dedicate this thesis to my parents and lovely youngest sister Nehdia, whom I increasingly miss with every passing moment, particularly ten years after they departed to Heaven.

TABLE OF CONTENTS

LIST OF FIGURES

LIST OF TABLES

LIST OF MAPS

Map pocket

CRUSTAL STRUCTURE OF THE SULAIMAN RANGE, PAKISTAN, FROM GRAVITY DATA

INTRODUCTION

The Sulaiman Range is part of the fold-and-thrust system along the western margin of the Indo-Pakistani plate. This system is conspicuous because of its widespread extent over the foreland, primarily due to effective decoupling of the sedimentary sequence from the underlying basement (Seeber and Armbruster, 1979). The 250 km wide Sulaiman lobe is bounded to the northwest and north by the Zhob Thrust and Katawaz flysch basin, to the northeast, east and southeast by the Indus plain constituting the Sulaiman foredeep, and to the southwest and west by the Sibi syntaxis (fig. 1).

Like the other fold-and-thrust belts of Pakistan (Kashmir, Salt Range/Potwar Plateau, Kirther Range), the Sulaiman Range is a consequence of the convergence of the Indo-Pakistani and Eurasian plates that resulted in the ongoing Himalayan collision. Knowledge about the deep structure of the Himalayan convergence zone has been advanced as a result of extensive studies carried out by many workers. Particularly, gravity interpretations by Marussi (1964, 1976, 1980), Karner and Watts (1983), Verma and Subrahmanyam (1984), Lyon-Caen and Molnar (1983, 1985), Duroy (1986), and Malinconico (1986, 1989) provide ideas about the nature and structure of the crust underneath the high Himalayan mass. In northern Pakistan the crust is nearly twice normal continental thickness (~70 km). To the south, in the Salt Range and Potwar Plateau region (fig. 1), a maximum of 7 to 8 km of sediments are thrust over full-thickness continental crust (Duroy et al., 1989). However, in the Sulaiman region, little is known about the underlying crust.

The Sulaiman region depicts a complex interaction of strike slip and thrust motion, owing to oblique convergence along the Chaman fault (Lawrence and Yeats, 1979; Lawrence et a l., 1981; Farah et al., 1984). On the undisturbed craton, Mesozoic and younger sediments are about 2 km thick, but have been interpreted to thicken to > 15 km in the western part of the Sulaiman Range. (Banks and Warburton, 1986). Seismic reflection profiles show the basement to be more than 10 km deep beneath frontal folds of the Sulaiman Range (Humayon et al., 1991; Jadoon et al., 1991). However, the lines do not extend far enough to constrain basement depths beneath the interior of the range.

An east-west gravity profile was evaluated in this thesis to study the configuration of the top of the basement as well as the Moho. The nature of these boundaries beneath the interior of the Sulaiman Range has helped in interpreting the overall nature and structure of the crust along the western margin of the Indo-Pakistani plate.

In contrast to large negative Bouguer gravity anomalies in the Pakistan Himalaya (Malinconico, 1986, 1989; Duroy et al., 1989), relatively small negative Bouguer gravity anomalies are observed over the Sulaiman region (Rahman, 1969; Marussi, 1976). Modeling

Figure 1. Major tectonic features along the western and northwestern margins of the Indo-Pakistani plate (adapted from Humayon et al., 1990). Note the broad foldbelts in Pakistan suggesting weak decollement zones. Also note the emplacement of flysch and ophiolites near the Chaman Fault, marking the boundary zone between the Indo-Pakistani plate and the Afghan Block. The large arrow indicates the motion of the Indo-Pakistani plate relative to the Eurasian plate. The Mari-Kandkot high (MK), Jacobabad high (JB) and the Talhar Fracture Zone (TFZ) are structures that may indicate the northward continuation of the western passive margin of the Indo-Pakistani plate under the Indus alluvium and the Kirthar and Sulaiman foldbelts (Quadri and Shuaib, 1986; Malik et al., 1989). The Sargodha basement high (SG) is a flexural bulge (Duroy et al., 1989), due to loading by the Himalaya. Line Y-Y' is the gravity profile interpreted in this study. Rectangle shows the area covered in figure 2.

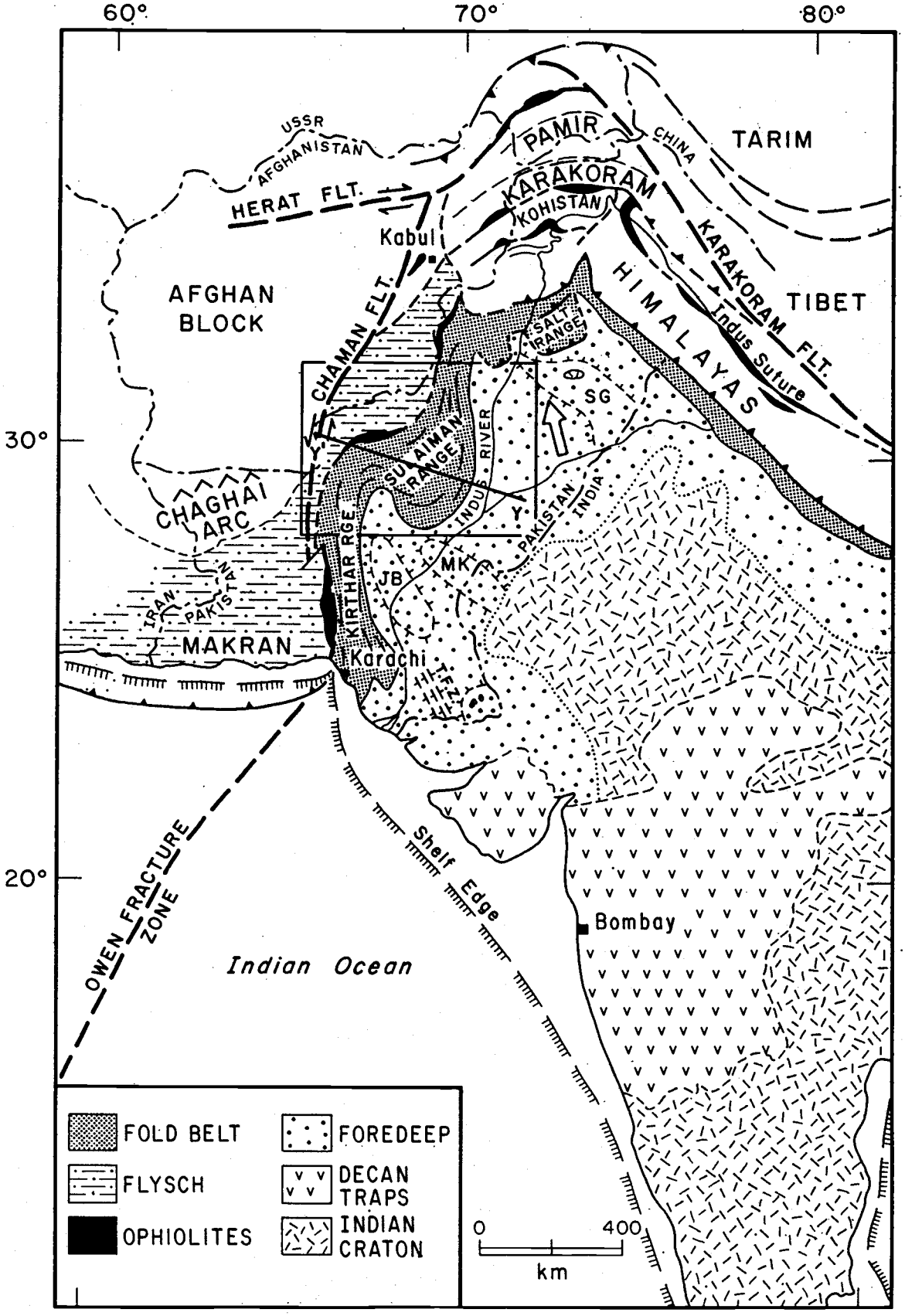
60°
70°
80°
30°
20°
USSR
AFGHANISTAN
PAMIR
CHINA
TARIM
HERAT FLT.
KARAKORAM
KOHISTAN
KARAKORAM FLT.
Kabul
AFGHAN BLOCK
CHAMAN FLT.
SALT RANGE
HIMALAYAS
Indus Suture
TIBET
SG
SULAIMAN RANGE
INDUS RIVER
CHAGHAI ARC
KIRTHAR RGE
PAKISTAN
INDIA
JB
MK
IRAN
PAKISTAN
MAKRAN
Karachi
HT
HTN
HT
OWEN FRACTURE ZONE
Shelf Edge
Bombay
Indian Ocean
FOLD BELT
FLYSCH
OPHIOLITES
FOREDEEP
DECAN TRAPS
INDIAN CRATON
0
400
km

FIGURE 1

in this thesis suggests that the thick, low density sediments are compensated by shallow mantle material in the Sulaiman region, implying that the underlying crust is transitional in thickness between that of normal continental and oceanic crust. Thus, passive margin structures, identified in the Cambay region and lower Indus Basin (Naini and Talwani, 1983; Malik et al., 1988), may continue underneath the Sulaiman fold and thrust system (fig. 1).

In the first part of this thesis free-air, Bouguer and Airy isostatic gravity anomalies are presented, and some important considerations regarding the Moho configuration and isostatic state of the region are discussed. These results, along with assumptions developed about the shallow crust, are then used as constraints for the construction of a two-dimensional gravity model. For this purpose, forward gravity modeling was done using the GM-SYS computer modeling program, based on the Talwani (1959) method and supplied by Northwest Geophysical Associates, Inc.

The preferred model is interpreted as a rifted continental margin involved in early stages of collision, by comparing the interpreted crustal structure with that of undeformed passive margins and other mountain belts. Finally, possible physical mechanisms responsible for deformation in the region are discussed and a tectonic model, based on the preferred 2-D gravity model, is proposed.

REGIONAL TECTONIC AND GEOLOGICAL SETTING

Fold-and-thrust belts over the Himalayan foreland in Pakistan are the products of the ongoing collision between the Indo-Pakistani and Eurasian plates (fig.1). Continent-continent collision, which led to the building of the Himalayan Ranges, is considered to have begun in the middle Eocene (Molnar and Tapponier, 1975; Powell, 1979). The Himalayan mountain belt changes strike from northwest-southeast in India to east-west in Pakistan. The foreland fold-and-thrust structures are conspicuously broader in Pakistan than in India, particularly the Salt Range/Potwar Plateau and the Sulaiman fold belt. This difference is generally attributed to the presence, in Pakistan, of a thick evaporite sequence that acts as a weak decollement between the sedimentary cover and underlying basement (Seeber and Armbruster, 1979; Lillie et al., 1987; Jaume and Lillie, 1988).

The Sulaiman and Kirther ranges (fig. 1) represent the foreland fold-and-thrust belt along the northwestern margin of the Indo-Pakistani plate, bounded by the left-lateral Chaman transform zone in the west and the Indus plain on the east side (Abdel-Gawad, 1971; Lawrence et al., 1981). The broad width (250 km) of the Sulaiman Range (fig. 2) suggests that the range is a thin-skinned structure, thrusting southward on a weak decollement above a low angle, northwestward dipping basement (Sarwar and DeJong, 1979; Seeber et al., 1981; Humayon et al., 1991). However, it is not known if the decollement is an extension of the weak Eocambrian evaporite zone known to underlie the Salt Range/Potwar Plateau region, or if it is another type of weak zone.

Structural complexities in the Sulaiman region owe their origin to oblique convergence of the Indo-Pakistani plate along the Chaman fault system, which transforms motion between the Makran subduction zone, in the south, and the Himalayan convergence zone to the north (fig. 1, Lawrence et al., 1981; Farah et al., 1984). Some of the pre-existing basement structures (Mari-Kankot and Jacobabad highs), which may have developed as passive margin structures along the western edge of the Indo-Pakistani plate during Mesozoic rifting of Gondwana (Chaudary, 1975; Naini and Talwani, 1983; Quadri and Shuaib, 1986; Malik et al., 1988), may also influence the structural development of the Sulaiman Range.

In general, rocks exposed in the Sulaiman area can be divided into three main groups to emphasize their tectonic significance (Raza et al., 1989). From east to west, along the gravity profile (fig. 2), these units are: (1) Late Oligocene to Recent molasse deposited at the deformation front; (2) Permian to Eocene, shallow marine shelf to deep marine rocks exposed in the fold belt area (Kazmi and Rana, 1982); and (3) late Eocene to early Oligocene Khojak Flysch (Lawrence and Khan, 1990), deposited between the Chaman transform fault to the west and the Muslimbagh ophiolite in the east. These later sequences are thrust over Mesozoic-Cenozoic shelf strata, along a number of thrust faults in the Zhob valley (Abbas and

Figure 2. Map of the Sulaiman foldbelt showing the major tectonic features and some of the anticlinal structures at the deformation front (modified from Humayon et al., 1991). A-A' is the location of the cross section interpreted by Humayon et al. (1991) and B-B' is the position of the cross section interpreted by Jadoon et al. (1991). C-C' and D-D' are the locations of the cross sections made by Banks and Warburton (1986). Y-Y' is the gravity profile interpreted in figures 4 to 7, and the broken lines from D. G. Khan to Chaman are the actual gravity transects done by the Geological Survey of Pakistan (see map, Map pocket A).

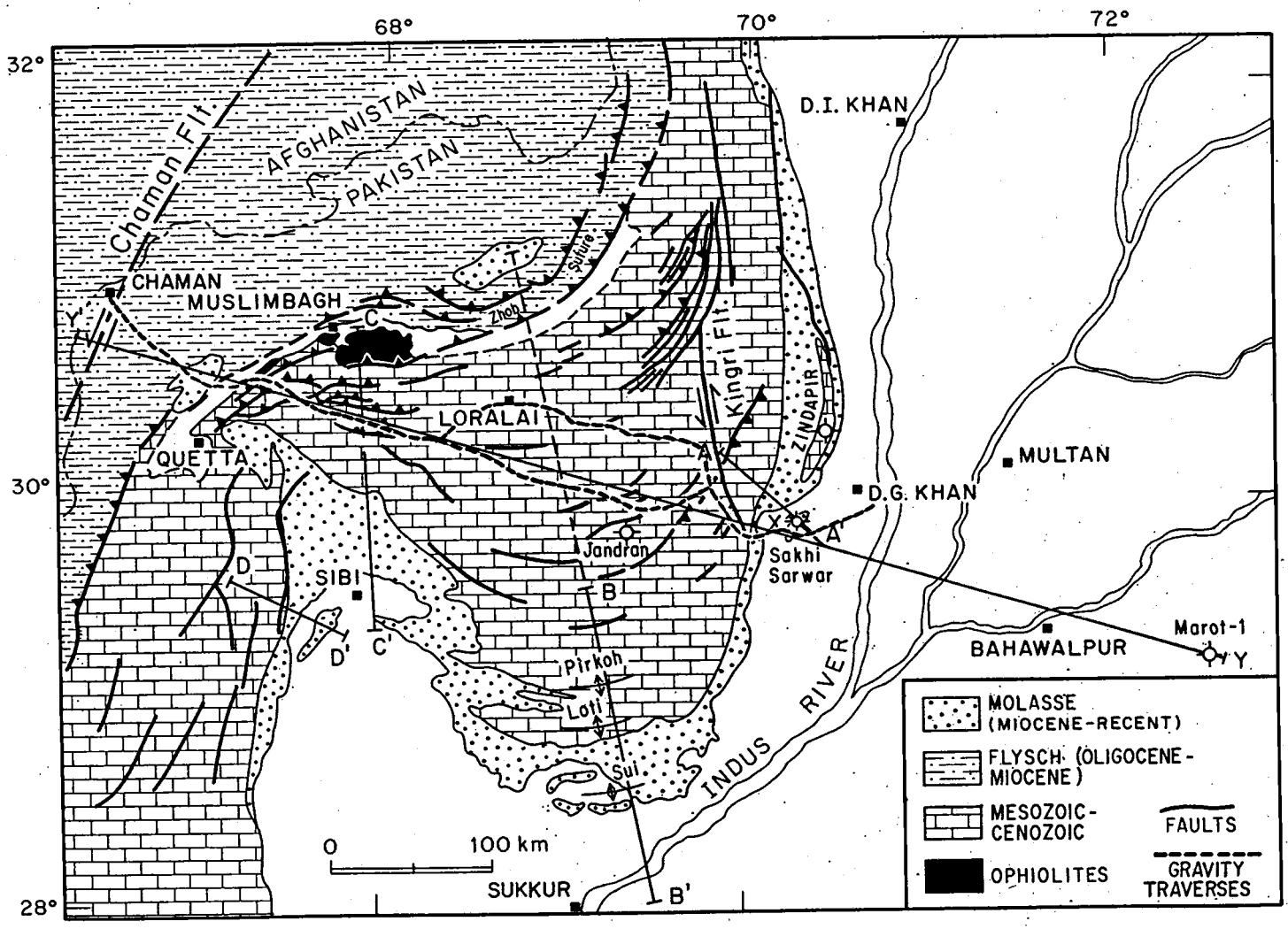
68°
70°
72°
32°
30°
28°
AFGHANISTAN
PAKISTAN
Chaman Fl.
CHAMAN
MUSLIMBAGH
QUETTA
LORALAI
SIBI
Zhob
Suture
Kingri Fl.
ZINDAPIR
D.I. KHAN
MULTAN
D.G. KHAN
Jandran
Sakhi Sarwar
BAHAWALPUR
Marot-1
Pirkoh
Loti
Sui
INDUS RIVER
SUKKUR
0
100 km
A
A'
B
B'
C
C'
D
D'
X
Y
Y'
MOLASSE (MIOCENE-RECENT)
FLYSCH (OLIGOCENE-MIOCENE)
MESOZOIC-CENOZOIC
OPHIOLITES
FAULTS
GRAVITY TRAVERSES

FIGURE 2

Ahmad, 1979). Ophiolites are present all along the eastern (Sengupta et al., 1990), northern (Gansser, 1980), and western (Gansser, 1980; Lawrence et al., 1981) convergence boundaries of the Indo-Pakistani plate. In the west they probably continue underneath the Khojak Flysch as remnants of Neotethys oceanic crust (Farah and Zaigham, 1979).

Figure 3 gives the general stratigraphy of the Sulaiman fold belt and foredeep region, based on surface geology, well data and seismic reflection profiles (Humayon et al., 1991; Jadoon et al., 1991). In the foredeep area, a 2 km thick, Precambrian to Recent sedimentary sequence is encountered in the Marot well (fig. 2, Humayon et al., 1991). A major stratigraphic break occurs between the Cambrian and Permian sequences (Raza et al., 1989). The Cambrian sequence, marine in origin, thins out in the west, suggesting easterly tilting of the platform during that time. In contrast, the Mesozoic and younger strata thicken to >10 km to the west. Both the Mesozoic and younger strata, predominantly comprised of carbonates, sandstone and shale with facies changes toward the east, suggest typical shelf environments (Malik et al., 1988; Raza et al., 1989; Humayon et al., 1991). In the fold belt, exposures are generally older toward the west as the strata are uplifted 4 to 8 km from their regional level as a result of duplex geometry (fig. 2; Banks and Warburton, 1986; Humayon et al., 1991; Jadoon et al., 1991). On the western side of the foldbelt Khojak Flysch (dominantly deep water turbidities) and ophiolites are present (Lawrence et al., 1981).

Facies changes in the Mesozoic-Cenozoic sedimentary sequences, from west to east and north to south (fig. 2), indicate deep marine to shallow water shelf environments, reflecting evolution of a passive continental margin during Mesozoic time. Collision processes from Paleocene to Recent time were accompanied by emplacement of the ophiolite along the western margin of the Indo-Pakistani plate (Lawrence et al., 1981).

Figure 3. Generalized stratigraphy of the Sulaiman foldbelt and foredeep (adapted from Humayon et al., 1991). Thicknesses in the foldbelt and foredeep are shown along with interval velocities encountered in the foredeep area, on the basis of which sediment densities (Table 3) are approximated for the present study.

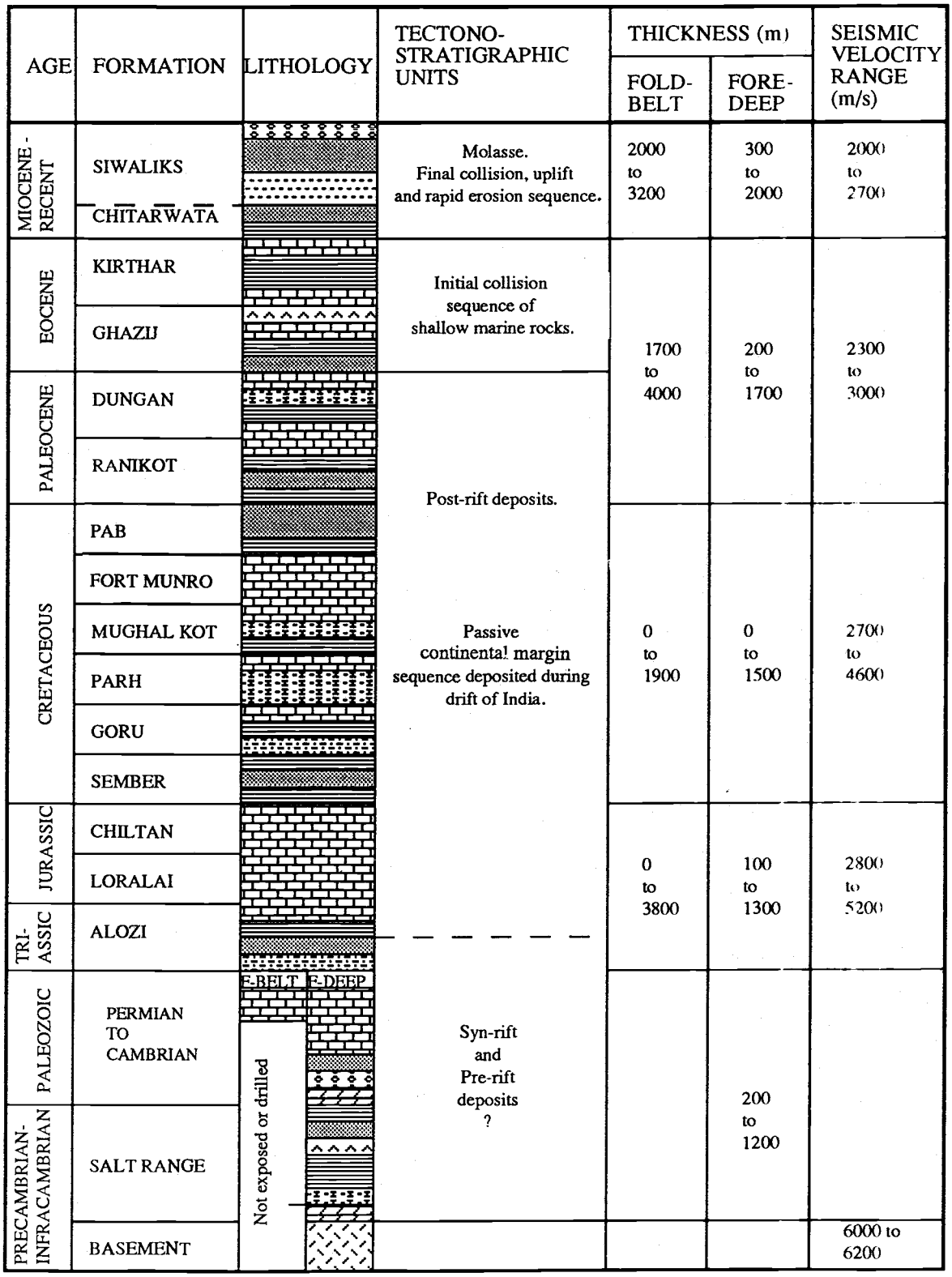
AGE
FORMATION
LITHOLOGY
TECTONO-STRATIGRAPHIC UNITS
THICKNESS (m)
FOLD-BELT
FORE-DEEP
SEISMIC VELOCITY RANGE (m/s)
MIOCENE - RECENT
SIWALIKS
CHITARWATA
Molasse. Final collision, uplift and rapid erosion sequence.
2000 to 3200
300 to 2000
2000 to 2700
EOCENE
KIRTHAR
GHAZIJ
Initial collision sequence of shallow marine rocks.
PALEOCENE
DUNGAN
RANIKOT
Post-rift deposits.
1700 to 4000
200 to 1700
2300 to 3000
CRETACEOUS
PAB
FORT MUNRO
MUGHAL KOT
PARH
GORU
SEMBER
Passive continental margin sequence deposited during drift of India.
0 to 1900
0 to 1500
2700 to 4600
JURASSIC
CHILTAN
LORALAI
TRI-ASSIC
ALOZI
0 to 3800
100 to 1300
2800 to 5200
F-BELT
F-DEEP
PALEOZOIC
PERMIAN TO CAMBRIAN
Not exposed or drilled
Syn-rift and Pre-rift deposits ?
200 to 1200
PRECAMBRIAN-INFRACAMBRIAN
SALT RANGE
BASEMENT
6000 to 6200

FIGURE 3

PREVIOUS WORK

Despite its intriguing structure and tectonic importance in the framework of crustal shortening along the Himalayan convergence zone, little geological/geophysical information is available on the Sulaiman area. Some geological mapping was undertaken by the Geological Survey of Pakistan, in collaboration with the Hunting Survey Corporation at a scale of 1:250,000 (Jones, 1961). Structural studies, predominantly based on LANDSAT images, seismicity and field studies, were done by Abdel-Gawad (1971), Menki and Jacob (1976), Rowlands (1978), Quittmeyer et al. (1979), Verma et al. (1980) and Hemphill and Kidwai (1973). These studies interpret the structure of the area as dominated by north-south trending, left-lateral strike slip faults and arcuate, compressional folds and faults. The axial orientation of the compressional features changes from east-west to north-south within the lobe. Banks and Warburton (1986) and Humayon et al. (1991) presented a passive roof duplex model to partly explain the enormous sedimentary thickness formed at the deformation front of the Sulaiman-Kirther ranges.

Rahman (1969) interpreted a 55 km thick crust, based on a gravity profile running along the road from Sukkur to Chaman, via Sibi and Quetta (fig. 2). Bouguer anomalies generally decrease from about -50 mgals in the Indus basin in the east to about -200 mgals at the Chaman fault, and then increase to -50 mgals over Afghanistan to the west (McGinnis, 1971; Marussi, 1976, see his plate 2). In contrast to the interpretation of Rahman (1969), who was unaware of the great thickness of the sedimentary wedge, the gravity behavior might be attributable to the deepening of the sedimentary section, accompanied by shallowing of the Moho from east to west (as discussed later in this thesis). On a smaller scale, positive Bouguer gravity anomalies in the Zhob area have been attributed to scattered, thin-skinned ophiolite bodies and partly to shallowing of the Moho (Farah and Zaigham, 1979). In addition, some earthquake studies were carried out by Menki and Jacob (1976), Molnar and Tapponnier (1978), Rowlands (1978), Seeber and Armbruster (1979), Verma et al. (1980), and others supporting active tectonics in the region. Surface waves studies by Chun (1986) suggest that the lithosphere beneath the Sulaiman Range has an oceanic affinity.

No other large-scale geophysical work has been reported in the Sulaiman area, except for proprietary seismic reflection and gravity surveys carried out by oil companies in the Sulaiman foredeep. Some of these data have been utilized as surface and subsurface constraints for this study.

DATA COLLECTION AND REDUCTION

In order to interpret the gross density structure of the Sulaiman region, gravity traverses were run along roads from D. G. Khan to Chaman by the Geological Survey of Pakistan (fig. 2). The traverses map (Map pocket A) depicts the location and terrain corrected Bouguer gravity value of each station, observed at 2 to 2.5 km intervals. Table 1 shows the observed gravity values and elevations, and the corresponding free-air and Bouguer gravity anomalies for each station. To the east, between D. G. Khan and Marot, the gravity contours on the map (Map pocket A) were incorporated from the Bouguer gravity map of AMOCO Pakistan Exploration Company (1972). The observed Bouguer gravity values are projected on profile Y-Y' running almost parallel to the roads (Table 2 and Map pocket A). Gravity values were projected to 5 km intervals and in total 115 Bouguer gravity values are utilized in this thesis study.

Gravity data obtained along the D. G. Khan-Chaman traverses were tied to local gravity base stations and subsequently reduced to the international gravity base at Karachi Airport (24^0 53' 54" N, 67^0 09' 12" E). The Bouguer gravity values are calculated using the 1930 Geodetic Reference System and density value of 2.67 gm/cm^3. The elevation of each gravity station was measured by an altimeter and was considered correct within 5 m, as these values were tied to local triangulation points established by the Survey of Pakistan (see map, Map pocket A). Terrain corrections were also applied; however, they only range from 0 to 5 mgals. Terrain corrected Bouguer gravity values are shown on the map (Map pocket A). Along line Y-Y', the average elevation in the fold belt (km marks 0 to 375 in Table 2) is about 1400 meters and in the foredeep it is just over 100 meters (km marks 380 to 575 in Table 2).

The Bouguer gravity values calculated agree well with the AMOCO (1972), and Marussi (1976) Bouguer gravity anomaly maps. However, considerable discrepancies occur with Bouguer gravity values of Rahman (1969), and Farah and Zaigham (1979) in the Chaman and Muslimbagh areas, respectively (fig. 2). Rahman did not mention what density he used for Bouguer reduction. However, the low Moho density contrast (0.15 gm/cm^3) used in this model to calculate crustal thickness, suggests that a reduction density higher than the standard 2.67 gm/cm^3 was used, leading to relatively low Bouguer gravity values. On the Farah and Zaigham (1979) profile the effect of high density mass lying on the surface appears to be dominant, because two reduction densities (2.6 and 2.8 gm/cm^3) were used for the Bouguer correction. However, gravity values do decrease towards the west and the crustal structure interpreted in the later study is consistent with the model presented in this thesis.

Table 1: Gravity data observed along roads from D. G. Khan to Chaman by the Geological Survey of Pakistan in 1988. Station numbers are shown on the map (Map pocket A). The Bouguer gravity values shown in the table are not terrain corrected. The asterisks denote gravity values based on previous observations by Qamar-ul-Huda of the Geological Survey of Pakistan in 1987.

Table 1

Chaman/D. G. Khan Road

Station No.	Observed Gravity (mgal)	Elevation (km)	Free-air Gravity (mgal)	Bouguer Gravity (mgal)
1	978.9543	1.494	+ 8	-159
2	978.9249	1.638	+ 24	-159
3	978.8939	1.792	+ 42	-156
4	978.8193	2.165	+ 77	-155
5	978.8764	1.910	+ 63	-151
6	978.8928	1.816	+ 51	-152
7	978.9069	1.724	+ 44	-155
8	978.9179	1.670	+ 37	-153
9	978.9284	1.605	+ 26	-153
10	978.9300	1.590	+ 24	-153
11	978.9369	1.546	+ 20	-153
12	978.9388	1.525	+ 16	-155
13	978.9329	1.513	+ 13	-156
14	978.9406	1.506	+ 12	-156
15	978.9406	1.491	+ 9	-157
16	978.9385	1.483	+ 1	-159
17	978.9332	1.468	- 1	-165
18	978.9324	1.468	- 1	-165
19	978.9317	1.465	- 2	-165
20	978.9307	1.460	- 3	-166
21	978.9290	1.459	- 4	-167
22	978.9271	1.460	- 5	-168
23	978.9258	1.464	- 6	-169
24	978.9241	1.450	- 12	-174
25	978.9231	1.460	- 9	-172
26	978.9220	1.463	- 9	-173
27	978.9201	1.471	- 9	-173
28	978.9194	1.480	- 7	-172
29	978.9197	1.485	- 4	-170
30	978.9199	1.487	- 2	-168
31	978.9220	1.501	+ 6	-162
32	978.9242	1.504	+ 9	-159
33	978.9192	1.508	+ 6	-163
34	978.9158	1.518	+ 7	-163
35	978.8815	1.673	+ 21	-166
36	978.8695	1.725	+ 25	-168
37	978.8476	1.796	+ 27	-174
38	978.8112	1.938	+ 37	-180
39	978.8199	1.929	+ 42	-173

(Table 1 cont.)

40	978.7893	2.078	+ 57	-175
41	978.7878	2.123	+ 57	-167
42	978.8186	1.976	+ 55	-166
43	978.8146	2.043	+ 71	-158
44	978.8052	2.091	+ 75	-158
45	978.7982	2.123	+ 78	-159
46	978.7847	2.187	+ 85	-159
47	978.7804	2.205	+ 87	-159
48	978.7724	2.242	+ 92	-159
49	978.7470	2.348	+102	-160
50	978.7313	2.440	+116	-156
51	978.7114	2.528	+123	-159
52	978.6895	2.638	+136	-159
53	978.7165	2.485	+117	-161
54	978.7310	2.409	+108	-161
55	978.7442	2.385	+114	-152
56	978.7552	2.301	+ 99	-158
57	978.7637	2.257	+ 94	-158
58	978.7734	2.234	+ 98	-152
59	978.7859	2.164	+ 90	-152
60	978.8009	2.103	+ 86	-148
61	978.8155	2.042	+ 83	-145
62	978.8280	1.990	+ 80	-144
63	978.8454	1.959	+ 78	-141
64	978.8498	1.895	+ 73	-139
65	978.8666	1.818	+ 66	-137
66	978.8722	1.788	+ 62	-137
67	-	1.723*	+ 67*	-125*
68	-	1.692*	+ 63*	-126*
69	-	1.631*	+ 56*	-126*
70	978.9233	1.569	+ 47	-129
71	-	1.473*	+ 43*	-122*
72	-	1.445*	+ 41*	-121*
73	-	1.357*	+ 35*	-117*
74	-	1.183*	+ 28*	-104*
75	-	1.174*	+ 28*	-103*
76	-	1.120*	+ 25*	-100*
77	-	1.105*	+ 22*	-101*
78	-	1.088*	+ 21*	-101*
79	-	1.073	+ 23*	- 97*
80	-	1.072*	+ 25*	- 95*
81	-	-	-	-
82	-	1.061*	+ 28*	- 91*
83	-	1.055*	+ 30*	- 88*
84	-	-	-	-
85	-	0.979*	+ 26*	- 83*
86	-	0.960*	+ 25*	- 82*
87	979.0752	0.957	+ 25	- 82
88	979.0775	0.950	+ 25	- 81
89	979.0766	0.954	+ 25	- 82
90	979.0773	0.955	+ 26	- 81

(Table 1 cont.)

91	979.0779	0.956	+ 27	- 80
92	979.0798	0.956	+ 28	- 78
93	979.0808	0.956	+ 30	- 77
94	979.0804	0.957	+ 29	- 78
95	979.0816	0.962	+ 32	- 76
96	979.0820	0.959	+ 32	- 76
97	979.0818	0.951	+ 30	- 76
98	979.0806	0.947	+ 28	- 78
99	979.0786	0.942	+ 26	- 80
100	979.0750	0.939	+ 22	- 83
101	979.0731	0.936	+ 20	- 85
102	979.0729	0.942	+ 23	- 83
103	979.0715	0.941	+ 22	- 83
104	979.0690	0.946	+ 21	- 85
105	979.0678	0.946	+ 21	- 85
106	979.0657	0.957	+ 22	- 85
107	979.0631	0.970	+ 23	- 84
108	979.0594	0.986	+ 25	- 85
109	979.0560	1.004	+ 27	- 85
110	979.0529	1.020	+ 29	- 85
111	979.0488	1.041	+ 32	- 84
112	979.0482	1.041	+ 31	- 85
113	979.0516	1.020	+ 28	- 86
114	979.0546	1.001	+ 24	- 87
115	979.0565	0.994	+ 24	- 87
116	979.0577	0.993	+ 25	- 86
117	979.0584	0.995	+ 26	- 85
118	979.0584	0.999	+ 27	- 85
119	979.0559	1.008	+ 27	- 85
120	979.0540	1.021	+ 30	- 84
121	979.0540	1.031	+ 33	- 82
122	979.0614	1.105	+ 72	- 51
123	979.0607	1.088	+ 67	- 54
124	979.0613	1.088	+ 67	- 54
125	979.0596	1.101	+ 69	- 54
126	979.0587	1.105	+ 69	- 55
127	979.0551	1.131	+ 73	- 54
128	979.0537	1.143	+ 74	- 54
129	979.0508	1.165	+ 77	- 53
130	979.0479	1.179	+ 77	- 54
131	979.0469	1.188	+ 79	- 54
132	979.0445	1.205	+ 81	- 54
133	979.0420	1.229	+ 85	- 53
134	979.0420	1.244	+ 88	- 51
135	979.0385	1.257	+ 88	- 53
136	979.0335	1.273	+ 88	- 55
137	979.0343	1.270	+ 86	- 56
138	979.0408	1.241	+ 83	- 56
139	979.0486	1.209	+ 81	- 54
140	979.0559	1.188	+ 81	- 52
141	979.0606	1.181	+ 83	- 49

(Table 1 cont.)

142	979.0722	1.135	+ 81	- 46
143	979.0770	1.120	+ 82	- 43
144	979.0770	1.108	+ 79	- 45
145	979.0783	1.094	+ 76	- 46
146	979.0789	1.084	+ 73	- 48
147	979.0855	1.090	+ 75	- 40
148	979.0748	1.140	+ 88	- 39
149	979.0472	1.276	+104	- 38
150	979.0065	1.494	+128	- 38
151	978.9781	1.608	+140	- 39
152	978.9774	1.603	+140	- 40
153	978.9985	1.472	+121	- 44
154	979.0402	1.326	+ 94	- 47
155	979.0623	1.128	+ 76	- 50
156	979.0797	1.067	+ 73	- 46
157	979.0874	1.025	+ 68	- 46
158	979.0962	0.942	+ 50	- 55
159	979.1181	0.808	+ 33	- 57
160	979.1197	0.772	+ 24	- 62
161	979.1307	0.648	- 05	- 75
162	979.1536	0.523	- 20	- 78
163	979.1496	0.509	- 28	- 85
164	979.1690	0.396	- 43	- 87
165	979.1764	0.348	- 50	- 89
166	979.1803	0.326	- 54	- 91
167	979.1852	0.300	- 58	- 92
168	979.1891	0.268	- 64	- 94
169	979.1846	0.264	- 70	- 99
170	979.1885	0.215	- 81	-105
171	979.1892	0.180	- 92	-112
172	979.1912	0.151	- 99	-116
173	979.1932	0.125	-107	-121
174	979.1951	0.122	-108	-122

(Table 1 cont.)

Table 1 (cont.)

Loralai/Rakhini Road

Station No.	Observed Gravity (mgal)	Elevation (km)	Free-air Gravity (mgal)	Bouguer Gravity (mgal)
175	-	1.635*	+ 63*	-120*
176	-	1.662*	+ 67*	-119*
177	-	1.656*	+ 69*	-116*
178	-	1.610*	+ 66*	-114*
179	-	1.503*	+ 58*	-110*
180	-	1.464*	+ 55*	-109*
181	-	1.430*	+ 53*	-107*
182	-	1.424*	+ 53*	-106*
183	-	1.400*	+ 52*	-104*
184	-	1.385*	+ 54*	-101*
185	-	1.363*	+ 54*	- 98*
186	979.0044	1.334	+ 46	-102
187	979.0064	1.323	+ 46	-102
188	979.0107	1.316	+ 48	-100
189	979.0144	1.308	+ 49	- 97
190	979.0179	1.302	+ 50	- 95
191	979.0231	1.290	+ 51	- 93
192	979.0275	1.279	+ 52	- 91
193	979.0298	1.275	+ 53	- 89
194	979.0354	1.263	+ 55	- 86
195	979.0399	1.245	+ 54	- 85
196	979.0460	1.228	+ 55	- 82
197	979.0489	1.221	+ 56	- 80
198	979.0614	1.214	+ 66	- 69
199	979.0512	1.230	+ 60	- 77
200	979.0510	1.239	+ 62	- 76
201	979.0517	1.242	+ 63	- 75
202	979.0542	1.235	+ 64	- 74
203	979.0563	1.228	+ 63	- 74
204	979.0573	1.225	+ 63	- 74
205	979.0572	1.224	+ 63	- 74
206	979.0577	1.218	+ 61	- 75
207	979.0555	1.225	+ 61	- 76
208	979.0571	1.217	+ 60	- 76
209	979.0555	1.229	+ 61	- 76
210	979.0511	1.255	+ 65	- 76
211	979.0501	1.262	+ 65	- 76
212	979.0504	1.256	+ 64	- 76
213	979.0466	1.270	+ 64	- 74
214	979.0457	1.276	+ 65	- 77
215	979.0452	1.286	+ 68	- 75

(Table 1 cont.)

216	979.0408	1.315	+ 72	- 74
217	979.0378	1.330	+ 74	- 75
218	979.0355	1.417	+ 86	- 73
219	979.0371	1.342	+ 76	- 74
220	979.0334	1.362	+ 78	- 74
221	979.0121	1.467	+ 89	- 75
222	979.0082	1.485	+ 90	- 76
223	979.0150	1.452	+ 87	- 75
224	979.0342	1.365	+ 79	- 73
225	979.0332	1.349	+ 75	- 76
226	979.0362	1.329	+ 72	- 77
227	979.0422	1.300	+ 68	- 77
228	979.0438	1.300	+ 69	- 76
229	979.0356	1.350	+ 76	- 75
230	979.0520	1.264	+ 65	- 76
231	979.0449	1.306	+ 73	- 73
232	979.0440	1.313	+ 75	- 72
233	979.0413	1.320	+ 75	- 73
234	979.0493	1.252	+ 62	- 78
235	979.0491	1.241	+ 60	- 79
236	979.0460	1.263	+ 65	- 76
237	979.0400	1.291	+ 70	- 75
238	979.0315	1.330	+ 75	- 74
239	979.0268	1.354	+ 80	- 72
240	979.0244	1.357	+ 80	- 72
241	979.0273	1.330	+ 76	- 72
242	979.0334	1.290	+ 72	- 72
243	979.0405	1.266	+ 74	- 67
244	979.0452	1.253	+ 77	- 63
245	979.0530	1.214	+ 66	- 61
246	979.0597	1.189	+ 75	- 58
247	979.0689	1.159	+ 78	- 51
248	979.0710	1.138	+ 75	- 52
249	979.0729	1.122	+ 74	- 51
250	979.0776	1.104	+ 76	- 48
251	979.0800	1.092	+ 69	- 47

Table 2: Straight line (Y-Y') projection of gravity values between Chaman and Marot (see map, Map pocket A and fig. 2). X = 0 km distance is on the west end of the line Y-Y'. Gravity values are projected at 5 km intervals; Z = elevation in km; F.A = Free-air anomaly in mgals; B.A = Bouguer anomaly in mgals; I.A = Airy isostatic anomaly in mgals.

Table 2

Foldbelt

X (km)	Z (km)	F.A (mgal)	B.A (mgal)	I.A(mgal)
0	1.493	+ 08	- 158	+ 12
5	1.637	+ 24	- 157	+ 14
10	2.165	+ 77	- 151	+ 20
15	1.815	+ 51	- 151	+ 20
20	1.605	+ 26	- 152	+ 20
25	1.546	+ 20	- 153	+ 20
30	1.505	+ 12	- 156	+ 17
35	1.483	+ 1	- 159	+ 14
40	1.468	- 1	- 165	+ 9
45	1.460	- 3	- 166	+ 8
50	1.460	- 5	- 168	+ 7
55	1.462	- 9	- 173	+ 3
60	1.485	- 4	- 169	+ 8
65	1.505	+ 6	- 162	+ 16
70	1.518	+ 7	- 163	+ 16
75	1.509	+ 7	- 162	+ 18
80	1.524	+ 9	- 162	+ 20
85	1.672	+ 21	- 166	+ 17
90	1.725	+ 25	- 168	+ 17
95	1.795	+ 27	- 173	+ 13
100	1.937	+ 37	- 173	+ 15
105	1.928	+ 42	- 173	+ 16
110	2.080	+ 57	- 175	+ 16
115	2.122	+ 70	- 163	+ 29
120	1.975	+ 55	- 162	+ 31
125	2.122	+ 78	- 157	+ 37
130	2.204	+ 87	- 155	+ 39
135	2.240	+ 91	- 154	+ 40
140	2.347	+102	- 155	+ 39
145	2.527	+123	- 154	+ 39
150	2.637	+136	- 154	+ 38
155	2.408	+109	- 155	+ 36
160	2.300	+ 99	- 154	+ 35
165	2.260	+ 94	- 155	+ 32
170	2.163	+ 90	- 150	+ 34
175	2.041	+ 83	- 145	+ 36
180	1.958	+ 78	- 142	+ 36
185	1.894	+ 73	- 139	+ 35
190	1.788	+ 62	- 136	+ 34
195	1.722	+ 67	- 125	+ 41
200	1.631	+ 56	- 126	+ 36
205	1.634	+ 63	- 120	+ 37
210	1.445	+ 41	- 121	+ 32

(Table 2 cont.)

215	1.356	+ 35	- 117	+ 31
220	1.183	+ 28	- 104	+ 40
225	1.072	+ 25	- 95	+ 45
230	1.055	+ 30	- 90	+ 46
235	0.950	+ 25	- 89	+ 43
240	0.960	+ 25	- 84	+ 45
245	0.955	+ 26	- 82	+ 44
250	0.962	+ 31	- 75	+ 46
255	0.963	+ 34	- 73	+ 47
260	0.966	+ 38	- 70	+ 48
265	0.963	+ 34	- 73	+ 43
270	0.962	+ 30	- 75	+ 39
275	0.960	+ 32	- 75	+ 37
280	0.947	+ 28	- 77	+ 34
285	0.942	+ 25	- 76	+ 34
290	0.930	+ 30	- 75	+ 33
295	0.945	+ 32	- 74	+ 33
300	0.960	+ 34	- 73	+ 34
305	0.960	+ 33	- 74	+ 32
310	0.945	+ 31	- 75	+ 30
315	0.930	+ 31	- 73	+ 31
320	0.960	+ 37	- 70	+ 34
325	1.006	+ 48	- 65	+ 38
330	1.128	+ 70	- 57	+ 45
335	1.088	+ 67	- 54	+ 47
340	1.273	+ 87	- 51	+ 49
345	1.134	+ 81	- 45	+ 53
350	1.092	+ 70	- 46	+ 50
355	1.400	+ 88	- 37	+ 56
360	1.480	+127	- 37	+ 53
365	1.600	+140	- 37	+ 49
370	1.024	+ 68	- 43	+ 39
375	0.771	+ 24	- 54	+ 24

(Table 2 cont.)

Table 2 (cont.)

Foredeep

X (km)	Z (km)	F.A (mgal)	B.A (mgal)	I.A(mgal)
380	0.396	- 43	- 73	+ 00
385	0.348	- 50	- 84	- 15
390	0.268	- 64	- 90	- 26
395	0.215	- 81	- 97	- 37
400	0.180	- 92	- 104	- 49
405	0.150	- 99	- 112	- 60
410	0.123	-107	- 116	- 68
415	0.116	- 97	- 110	- 65
420	0.114	- 96	- 109	- 67
425	0.113	- 95	- 108	- 68
430	0.113	- 94	- 107	- 69
435	0.111	- 93	- 106	- 70
440	0.111	- 93	- 106	- 72
445	0.110	- 92	- 105	- 72
450	0.110	- 90	- 102	- 70
455	0.110	- 85	- 97	- 67
460	0.110	- 80	- 92	- 63
465	0.110	- 76	- 88	- 60
470	0.110	- 72	- 84	- 57
475	0.110	- 70	- 82	- 55
480	0.110	- 68	- 80	- 54
485	0.108	- 66	- 78	- 53
490	0.108	- 63	- 75	- 50
495	0.108	- 61	- 73	- 49
500	0.108	- 60	- 70	- 49
505	0.108	- 58	- 70	- 47
510	0.108	- 58	- 70	- 48
515	0.107	- 57	- 69	- 47
520	0.107	- 57	- 69	- 47
525	0.107	- 55	- 67	- 46
530	0.107	- 52	- 64	- 43
535	0.107	- 51	- 63	- 43
540	0.107	- 50	- 62	- 42
545	0.107	- 49	- 61	- 41
550	0.107	- 46	- 58	- 39
555	0.107	- 40	- 52	- 33
560	0.107	- 33	- 45	- 26
565	0.107	- 27	- 39	- 21
570	0.107	- 22	- 34	- 16
575	0.107	- 18	- 30	- 12

DISCUSSION OF GRAVITY ANOMALIES

Figure 4 displays the gravity anomalies relative to each other and to topography, drawn at about eighty times vertical exaggeration. Numerical values relative to the same horizontal coordinates are shown in table 2.

Free-Air Gravity Anomalies

Free-air anomalies generally mimic the topography of an area, because compensation that occurs at a deep level yields a longer-wavelength effect (Heiskanen and Meinesz, 1958). The highest free-air gravity values (> +100 mgals) are observed in areas of high elevation in the foldbelt, while the lowest values (~ -100 mgals) are just east of the deformation front (near D. G. Khan), in the foredeep. Similar high free-air anomalies are observed at Fort Munro (+140 mgals) and at Ziarat (+136 mgals). Comparison of these anomalies to topography (1.6 km and 2.6 km, respectively) suggests some contribution from high density material at depth in the Fort Munro-Loralai area. On the western end of the profile, free-air gravity values are near zero, suggesting roots corresponding to topography produce isostatic compensation in this region.

Bouguer Gravity Anomalies

Bouguer gravity anomalies along profile Y-Y' generally decrease toward the west, with a low over the foredeep and high over the frontal Sulaiman Range, separated by a gradient of about 1.6 mgals/km. In the foredeep region, short-wavelength variations are primarily due to shallow-depth sedimentary structures, which are apparent on seismic reflection sections (Humayon et al., 1991). Values decrease to -116 mgals near D. G. Khan and abruptly increase to -37 mgals at Fort Munro. They remain relatively high for some distance to the west, decreasing slightly at a rate of about -0.3 mgals/km. Still farther west, between kilometer points 270 and 170, in the region west of Loralai, Bouguer anomalies decrease rapidly from -75 mgals to -155 mgals at a rate of about -1.0 mgal/km. West of the 170 km point the Bouguer gravity field is relatively flat, with three short-wavelength anomalies apparent.

Airy Isostatic Gravity Anomalies

To compute Airy isostatic anomalies, Bouguer anomalies were calculated that would result if the topography along the profile was compensated only by a crustal root (fig. 5). These computed anomalies were then subtracted from the observed Bouguer profile to yield the Airy Isostatic anomalies. For this purpose a 35 km thickness is assumed for 'normal' crust of the Indo-Pakistani plate. Roots were calculated by using densities of 2.7 gm/cm^3 for the

Figure 4. Gravity anomalies relative to elevation along gravity profile Y-Y'. Note that Bouguer anomalies are negative in the Sulaiman Range, while free-air and Airy isostatic anomalies are generally positive.

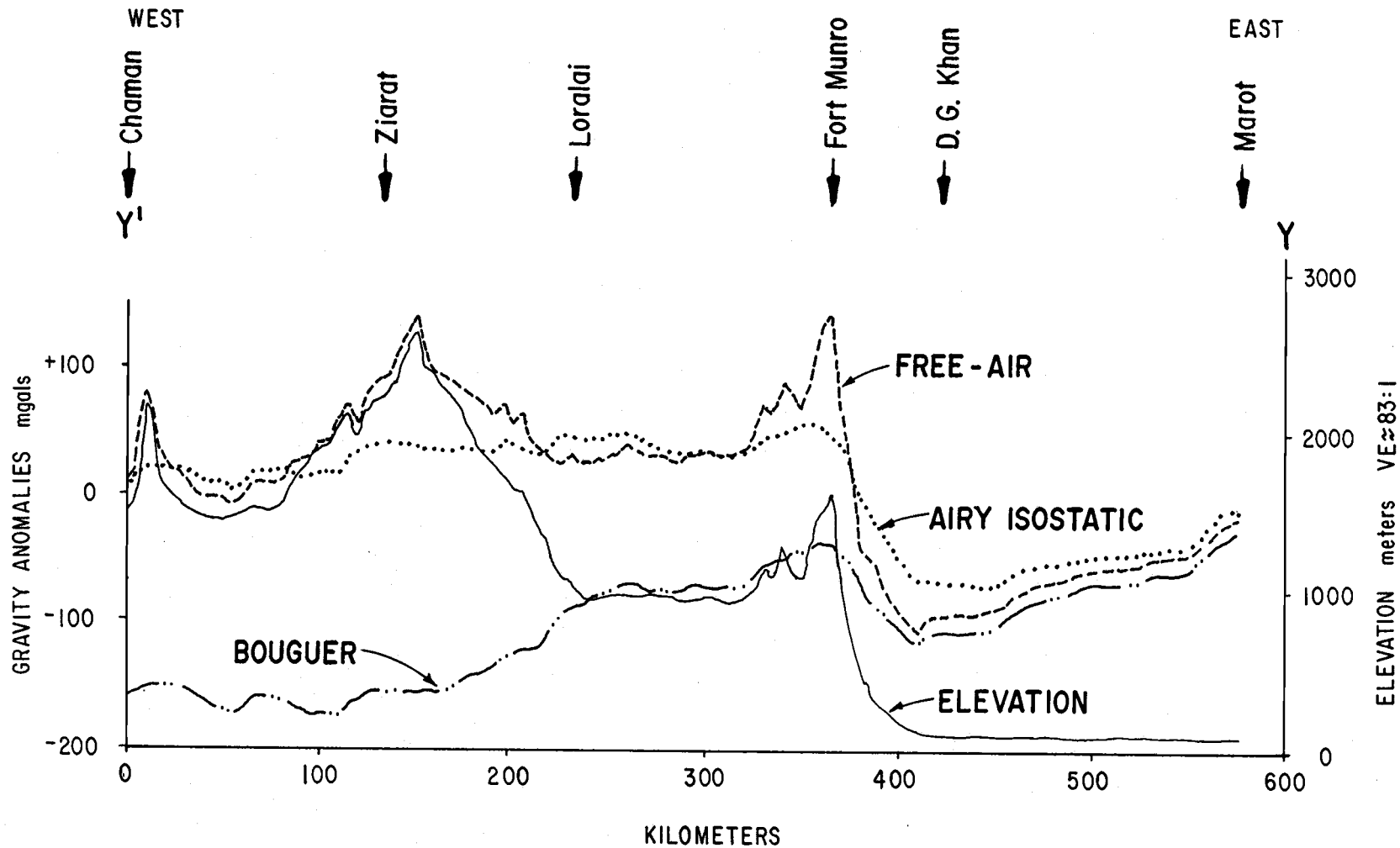
WEST
EAST
Chaman
Ziarat
Loralai
Fort Munro
D.G. Khan
Marot
Y'
Y
+100
0
-100
-200
GRAVITY ANOMALIES mgals
FREE-AIR
AIRY ISOSTATIC
BOUGUER
ELEVATION
3000
2000
1000
0
ELEVATION meters VE≈83:1
0
100
200
300
400
500
600
KILOMETERS

Figure 4

Figure 5. Roots calculated corresponding to surface topography, for normal crust of 35 km thickness at sea level, using Airy Isostatic compensation model. Compensation is assumed at 50 km depth at the base of the model. Assuming density 2.7 gm/cm^3 for the topography and crust, and 3.3 gm/cm^3 for the mantle, a density contrast of 0.6 gm/cm^3 is used across the Moho. Comparison of calculated root anomaly with observed Bouguer profile suggests that roots explain only parts of the observed profile. Subtraction of the calculated root anomaly from the observed Bouguer anomaly gives the Airy isostatic anomaly shown in fig. 4.

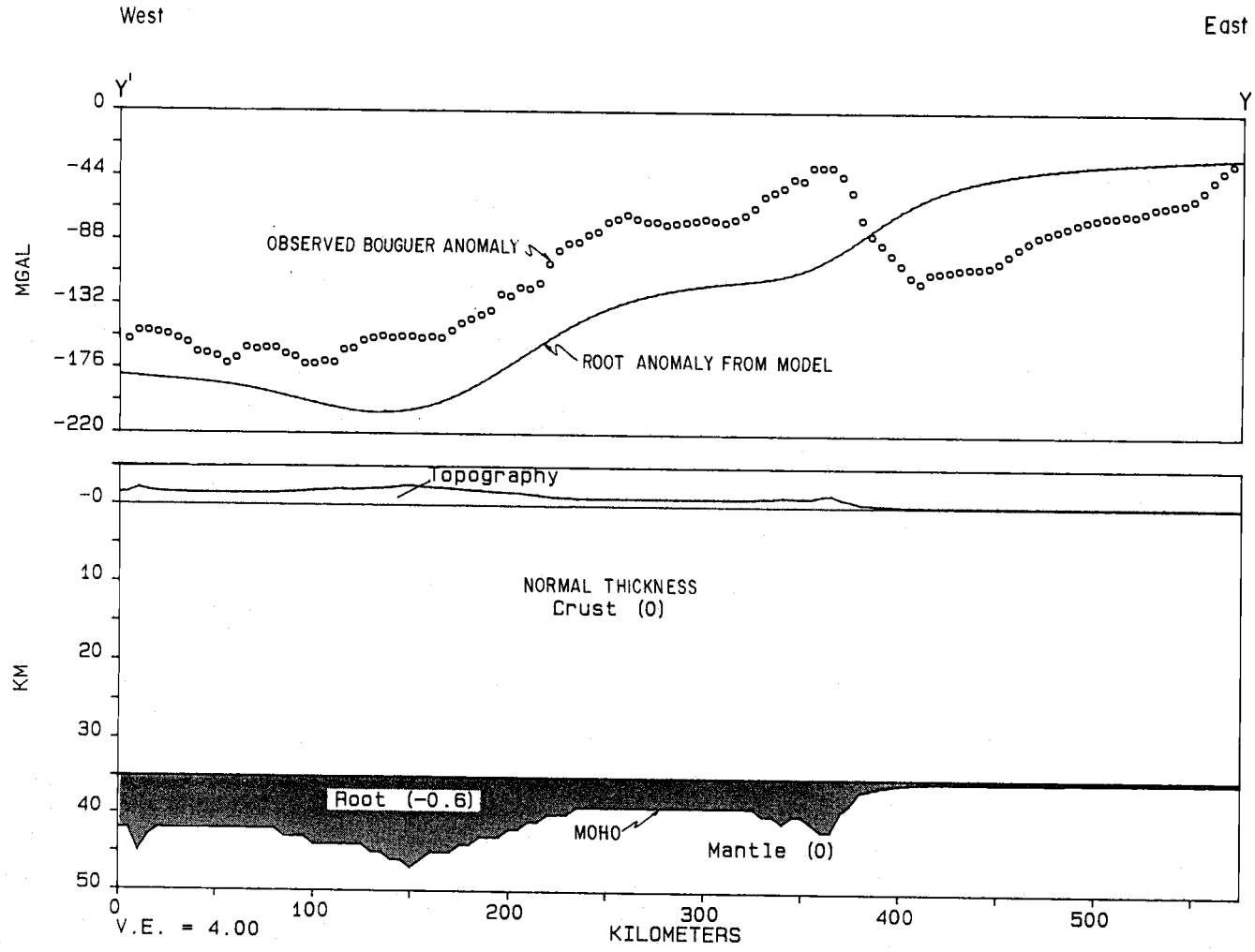
West
East
Y'
Y
0
-44
-88
-132
-176
-220
MGAL
OBSERVED BOUGUER ANOMALY
ROOT ANOMALY FROM MODEL
Topography
-0
10
20
30
40
50
KM
NORMAL THICKNESS
Crust (0)
Root (-0.6)
MOHO
Mantle (0)
0
100
200
300
400
500
V.E. = 4.00
KILOMETERS

FIGURE 5

crust and 3.3 gm/cm^3 for the upper mantle, which gives a density contrast of -0.6 gm/cm^3. The Airy compensation depth "H" from sea level is then calculated by:

$$H = T + 4.5h$$

where "T" is the normal crustal thickness and "h" is the height of the topography above sea level.

Isostatic gravity anomaly values in the area range from -72 mgals to +56 mgals, and the average value is +3 mgals, suggesting very general compensation of the area; however, there are zones that systematically deviate from equilibrium (fig. 4). Major patterns are a negative anomaly in the foredeep region, steep gradient between D. G. Khan and Fort Munro, a long-wavelength positive anomaly toward the west beyond 370 km, and various short wavelength anomalies.

The steep gradient that extends from about the 400 km point to the 370 km point separates low values over the foredeep from higher values over the frontal zone. The Airy isostatic anomaly values increase by 118 mgals over this zone. Similar isostatic gravity gradients are evident at many oceanic-continental boundaries (Rabinowitz and Labrecque, 1977).

In the foredeep region close similarity of short-wavelength anomalies with free-air and Bouguer gravity anomalies appears to be due to the dominance of structures at shallow depths. However, the isostatic anomaly is calculated by assuming the density contrast between the crust and mantle, and subtracting the root anomaly from the Bouguer gravity anomaly (fig. 5); deviations of the anomaly from zero may represent variations in Moho depth. In the Fort Munro-Loralai region the broad-wavelength positive isostatic anomaly may suggest undercompensation due to shallower than expected mantle material. It may be a southward extension of the shallow mantle identified in the Muslimbagh region (fig. 2; Farah and Zaigham, 1979), possibly inherited from Mesozoic rifting.

In the western extremity, beyond the 120 km point, the isostatic anomalies are near zero, suggesting local isostatic compensation of the region. Superimposed, three short-wavelength anomalies may represent a shallow, high density mass in the Ziarat region and isolated ophiolite bodies, in the subsurface, in the flysch basin region (Gansser, 1980; Farah and Zaigham, 1979).

The free-air anomalies also approach zero, beyond the 120 km point, west of Ziarat. The relatively low free-air values for such high topography at Ziarat may suggest mass deficiency in the deep subsurface. On the Bouguer anomaly, steep westward gradient, between kilometer points 270 and 170, suggests deepening of the Moho and subsequent thickening of the crust to the west. The short-wavelength Bouguer anomaly (positive isostatic

anomaly as well) present immediately at the lower end of the westward gradient, between 170-120 km points at Ziarat, is likely to be from a shallow source. Jurassic to Cretaceous rocks are exposed in the Ziarat region and topography is very high. It is possible that this shallow depth, high density source beneath Ziarat may be a basement high, While the remaining two short-wavelength anomalies are due to subsurface ophiolite bodies.

CONSTRAINTS

Since most of the major structures in the Sulaiman region are linear, 2-D modeling is a reasonable approach to interpret the Bouguer gravity anomalies observed in the area. The location of the profile was chosen purposely, keeping in mind the accessibility of the area and the work done and data used by Humayon et al. (1991). These data provide constraints for sediment thicknesses in the foredeep and frontal part of the Sulaiman fold belt. However, deep inside the fold belt area, control on sediment thickness can only be estimated from surface geology (Banks and Warburton, 1986; Humayon et al., 1991). Only in the area between Loralai and the western boundary of the Mesozoic sediments (approximately between the 100 and 250 km marks) are the structures strongly oblique to the section line. In this area, the 2-D modeling has some limitations.

At the Marot well (fig. 2) the basement is encountered at about 2 km depth and dips at about 2.5^{0} toward the west. Near the deformation front it is about 8 km deep and extends off the bottom of seismic lines at 5 sec two-way travel time (Humayon et al., 1991). Similarly, in the southern Sulaiman Range more than 15 km of sediments are interpreted near Jandran along line B-B' (Jadoon et al., 1991). If one extrapolates the basement surface deep inside the fold belt, assuming the same gentle dip along both the southern and eastern lines, it deepens to about 20 km near Loralai. This is consistent with the Banks and Warburton (1986) interpretation.

The Mesozoic-Cenozoic sediments are primarily composed of limestone, dolomite, sandstone, and shale, the densities of which generally vary between 2.17 to 2.75 gm/cm^3 (Dobrin and Savit, 1988). Interval velocities from seismic profiles (fig. 3), and lithologic descriptions and density logs from the Marot well (Humayon et al., 1991) provide estimates for the subsurface densities used in the gravity models. In addition, the Nafe and Drake (1957) curves (published in Sheriff, 1984), were utilized in estimating densities. Table 3 shows estimates of densities for different rock units encountered along the gravity profile.

The densities assumed for the upper and lower crust are 2.8 gm/cm^3 and 2.9 gm/cm^3 respectively. These values are below the density range determined by Chun (1986) for the western wedge of Indo-Pakistani crust. He determined shear wave velocities to be between 3.1 km/sec and 3.8 km/sec for the crust, which he associated with densities between 3.0 and 3.08 gm/cm^3, suggesting to him that the crust beneath the Sulaiman region has an oceanic affinity. On the same basis, densities Chun (1986) determined for the upper 10 km of sediments are between 2.66 and 2.72 gm/cm^3. These densities appear to be systematically high. Menki and Jacob (1976), Seeber and Armbruster (1979), and Kaila (1981), on the basis of earthquake seismic studies, interpreted P-wave velocities of 5.8 to 6.5 km/sec for the upper crust and 6.5 to 7 km/sec for the lower crust. Based on these values, the Nafe and

Table 3: Average densities of sedimentary rocks used for gravity models (fig. 6 and 7).

Geological Units	Age	Approximate velocity km/sec	Assumed Density gm/cm^3
Molasse	Miocene to Recent	2.0 - 2.7	2.1
Flysch	Oligocene to Miocene	-	2.65
Roofsediments (Cenozoic)	Eocene	2.3 - 3.0	2.55
Shelf sediments (Upper Paleozoic and Mesozoic)	Permian to Cretaceous	2.7 - 5.2	2.65
Ophiolites	?	-	2.8

Note: The P-wave velocities are obtained from Humayon et al.(1991), and the assumed densities are estimated according to Nafe and Drake (1957).

Drake (1957) curves suggest densities from 2.65 to 2.8 gm/cm^3 for the upper crust and 2.8 to 3.0 gm/cm^3 for the lower crust. P-wave velocities, determined in the above studies to range from 8 to 8.2 km/sec, suggest a density of 3.25 to 3.35 gm/cm^3 for the upper mantle.

Based on the above information, density contrasts of +0.4 gm/cm^3 between the lower crust and upper mantle, and -0.1 to -0.7 gm/cm^3 between sediments and upper crust were assumed for the 2-D models in this study. To compute the Airy isostatic anomaly, however, a simplified model of 2.7 gm/cm^3 for crust and 3.3 gm/cm^3 for mantle was assumed (fig. 5). The 0.6 gm/cm^3 contrast at the Moho thus yielded smaller roots than would have resulted if 0.4 gm/cm^3 was assumed.

GRAVITY MODELING

Assumptions and Limitations

A unique interpretation is almost impossible through gravity observations because of superimposed effects of many mass distributions; the free-air and Bouguer gravity fields represent the combined effects of shallow and deep sources. Isolated effects of each can only be determined if reasonable constraints are available. Since a primary objective of this study is to interpret the gross crustal structure and configuration of the Moho, some constraints and assumptions on the shallower crust had to be established. Sediment thicknesses west of the deformation front were estimated by assuming that the basement descends at about the same angle (2.5^{o}) observed at the deformation front, reaching a depth of about 20 km in the hinterland (Banks and Warburton, 1986).

A limitation is that the model is assumed to be 2-D, which is not entirely accurate because the line of section is oblique to the strike of the surface geologic structures in many places (fig. 2). Thus, a more thorough interpretation may require 3-D parameters, which is beyond the scope of the present study.

Construction of Models

In the foredeep region gravity anomalies are of low amplitude and there are no major differences between the free-air, Bouguer, and isostatic anomalies (fig. 4). Short-wavelength anomalies are caused by local structures identified on seismic profiles in the region (Humayon et al., 1991). West of the deformation front, positive free-air and isostatic anomalies suggest undercompensation, perhaps by mantle material that is shallower than expected in the region west of the 400 km point.

The comparison of observed Bouguer anomalies with the calculated root anomaly in figure 5 suggests that portions of the region are compensated in a manner that differs significantly from simple Airy isostatic equilibrium. Subtraction of the calculated root anomaly from the observed Bouguer anomaly in figure 5 thus yields the Airy isostatic anomaly shown in figure 4 and in Table 2. Figure 6 depicts a 2-D density model constructed using the above mentioned constraints, assumptions and the shape of the Moho from the crustal root calculated in figure 5. The anomaly calculated from the model shows a low toward the foreland and high over the hinterland. This anomaly is in agreement with the observed Bouguer anomaly in the eastern and western extremity of the gravity profile, but the long wavelength discrepancy in the region between the 500 km and 100 km points might suggest shallowing of the Moho to match the relatively high Bouguer anomaly. Figure 7 depicts the same 2-D density model as in figure 6, but with the Moho adjusted so that the observed and calculated Bouguer anomalies are in close agreement.

Figure 6. Comparison of the observed Bouguer anomaly and the calculated anomaly of the 2-D density model drawn, using the constraints and assumptions discussed in the text and the Moho depths obtained in figure 5. The difference between the observed and calculated anomalies might suggest that the mantle is shallower in the region between Km marks 100 and 450. Depth control west of Km mark 350 is poor and is based on: i) Banks and Warburton (1986) structural interpretation, ii) assuming that the basement is continuously deepening towards the west as it does on the seismic reflection lines in the foredeep and beneath the deformation front (Humayon et al., 1991; Jadoon et al., 1991). The basement high (km marks 120 to 170) is the same as that interpreted in the model (fig. 7). Ophiolite bodies are arbitrarily drawn to match the small wavelength anomalies. Density contrasts (gm/cm^3) for the sediments and mantle are relative to the crystalline crust.

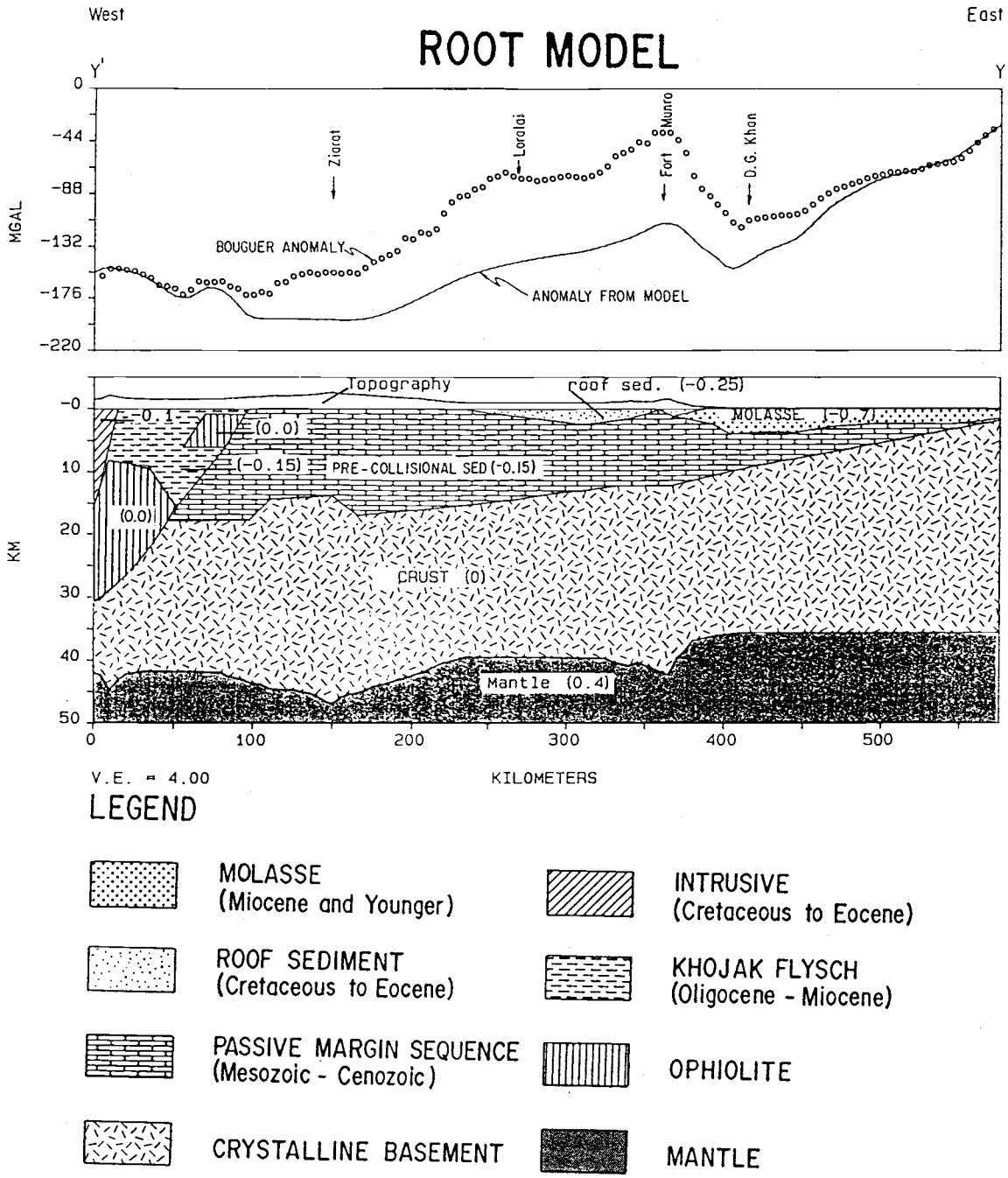
West
East
ROOT MODEL
Y'
Y
MGAL
0
-44
-88
-132
-176
-220
Ziarat
Loralai
Fort Munro
D.G. Khan
BOUGUER ANOMALY
ANOMALY FROM MODEL
KM
Topography
roof sed. (-0.25)
-0.1
(0.0)
MOLASSE (-0.7)
(-0.15)
PRE-COLLISIONAL SED (-0.15)
(0.0)
CRUST (0)
Mantle (0.4)
0
10
20
30
40
50
0
100
200
300
400
500
V.E. = 4.00
KILOMETERS
LEGEND
MOLASSE
(Miocene and Younger)
ROOF SEDIMENT
(Cretaceous to Eocene)
PASSIVE MARGIN SEQUENCE
(Mesozoic - Cenozoic)
CRYSTALLINE BASEMENT
INTRUSIVE
(Cretaceous to Eocene)
KHOJAK FLYSCH
(Oligocene - Miocene)
OPHIOLITE
MANTLE

FIGURE 6

Figure 7. Preferred 2-D density model showing the presence of transitional crust underneath the thick sediments of the Sulaiman foldbelt. The model shows relatively shallow Moho between 540 km point to 170 km point. To the west of the 170 km point, the Moho flattens at about 43 km depth. A 50 km wide basement high is interpreted between the 170 km and 120 km points. Sediments, density, basement constraints, ophiolite bodies, and the patterns shown are the same as in fig. 6. Figures 7a, b, and c, respectively, represent the shallow source, Moho, and cumulative effects. Density contrasts are relative to crystalline basement of assumed density 2.8 gm/cm^3 for the upper crust and 2.9 gm/cm^3 for the lower crust. Figure 7d shows the model with no vertical exaggeration.

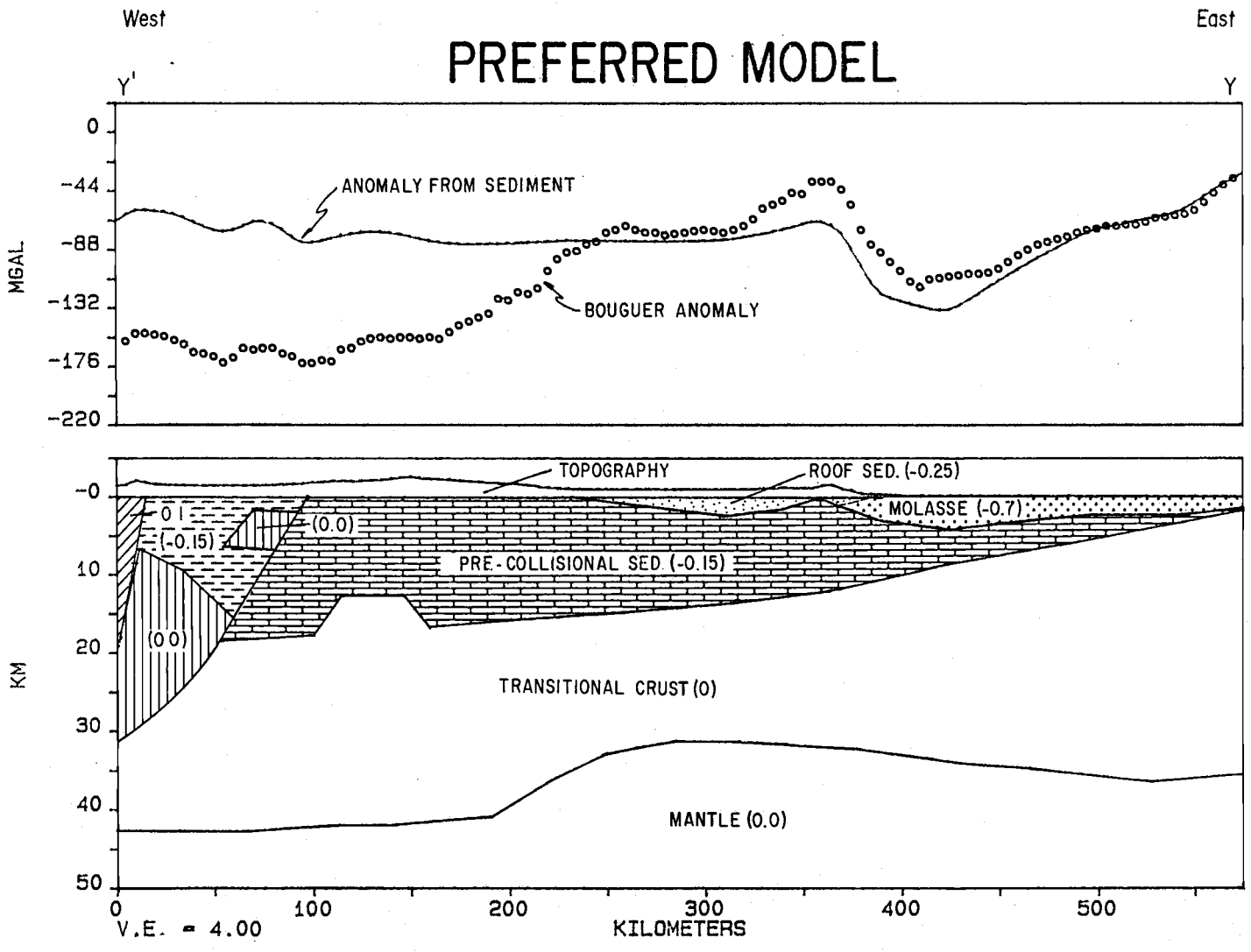
West
East
PREFERRED MODEL
Y'
Y
0
-44
-88
-132
-176
-220
MGAL
ANOMALY FROM SEDIMENT
BOUGUER ANOMALY
TOPOGRAPHY
ROOF SED. (-0.25)
MOLASSE (-0.7)
0
(-0.15)
(0.0)
PRE-COLLISIONAL SED. (-0.15)
(0.0)
TRANSITIONAL CRUST (0)
MANTLE (0.0)
KM
0
10
20
30
40
50
0
100
200
300
400
500
V.E. = 4.00
KILOMETERS

Figure 7a

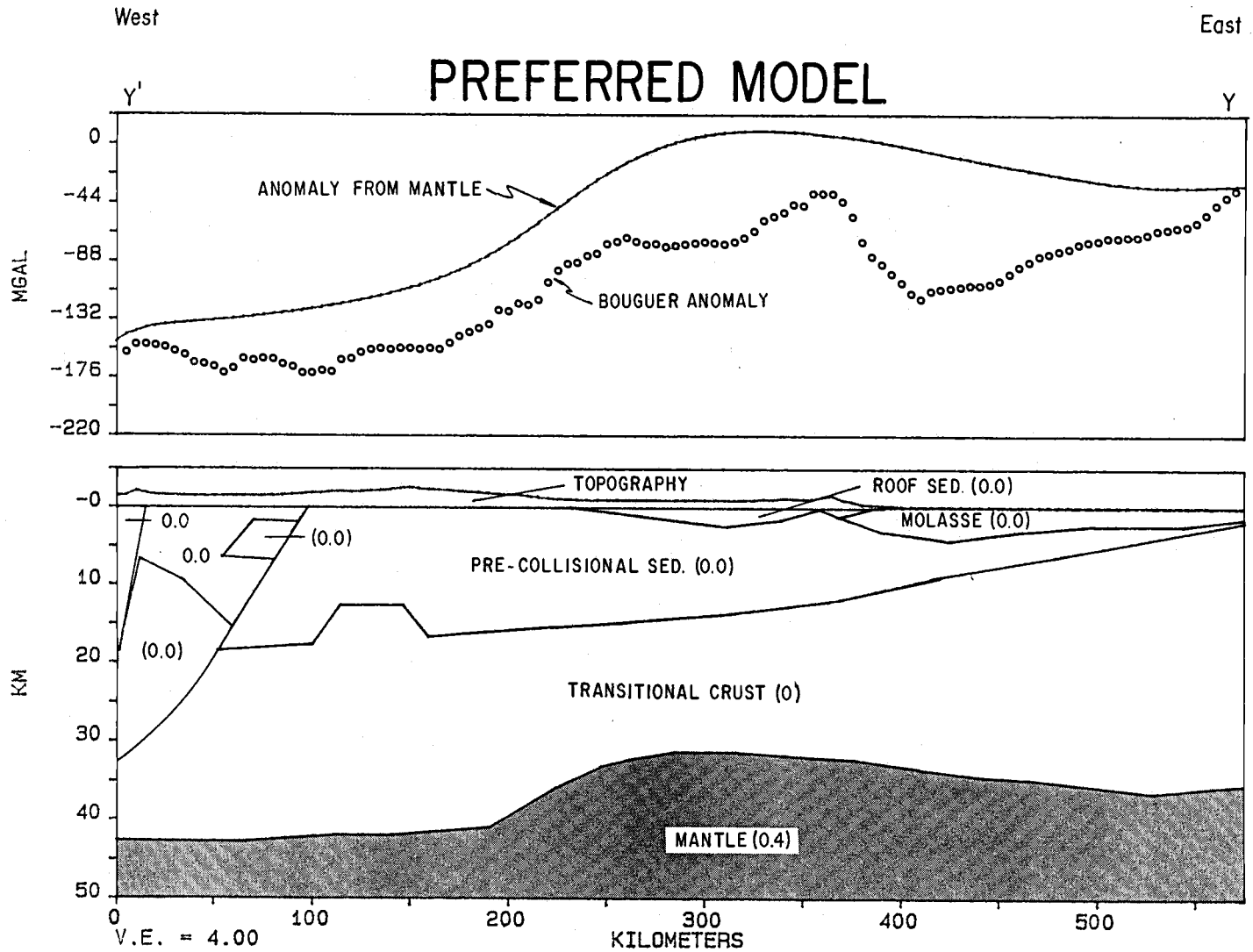
West
East
PREFERRED MODEL
Y'
Y
0
-44
-88
-132
-176
-220
MGAL
ANOMALY FROM MANTLE
BOUGUER ANOMALY
TOPOGRAPHY
ROOF SED. (0.0)
MOLASSE (0.0)
0.0
0.0
(0.0)
(0.0)
PRE-COLLISIONAL SED. (0.0)
TRANSITIONAL CRUST (0)
MANTLE (0.4)
KM
-0
10
20
30
40
50
0
100
200
300
400
500
V.E. = 4.00
KILOMETERS

Figure 7b

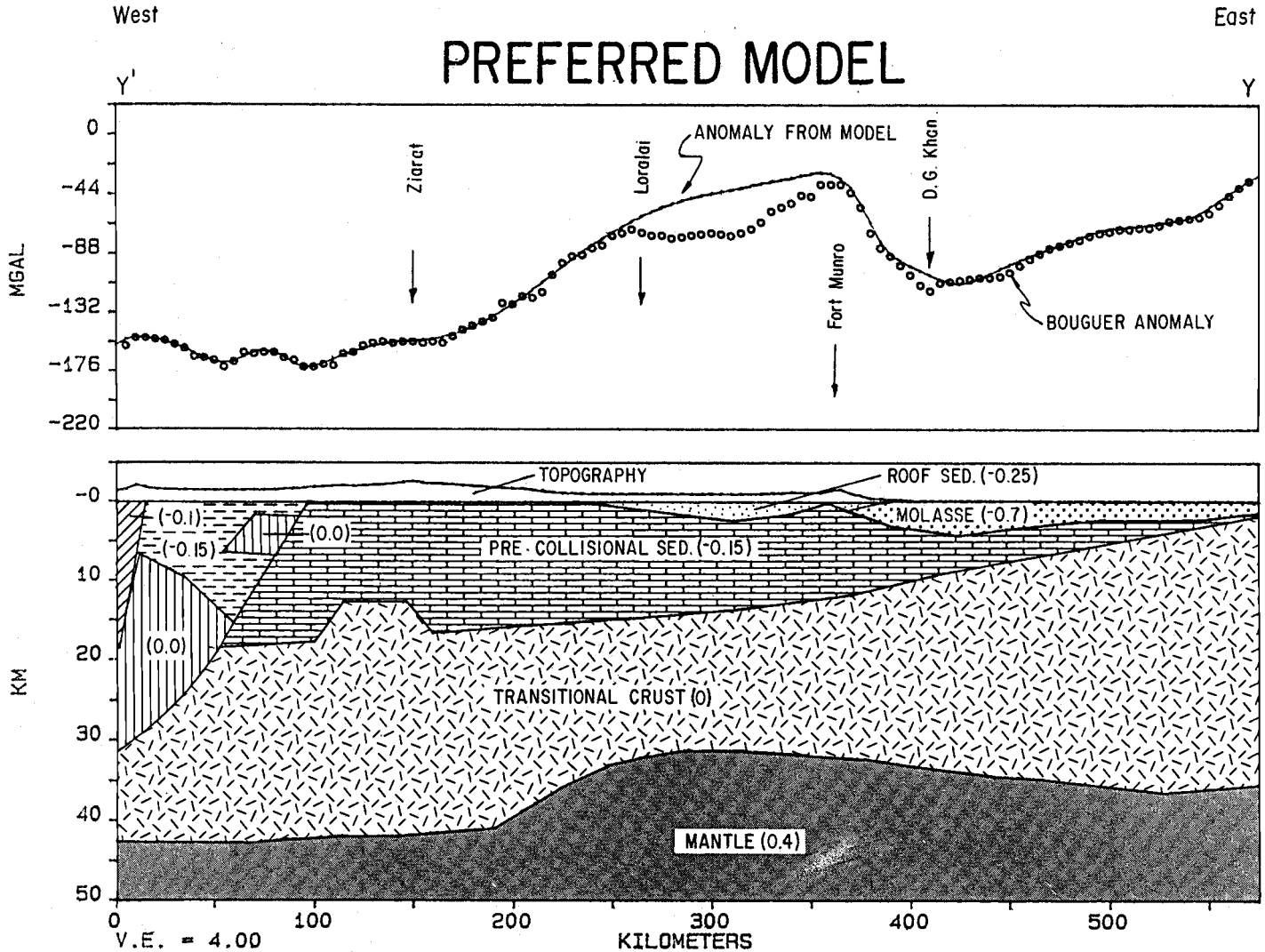
West
East
PREFERRED MODEL
Y'
Y
MGAL
0
-44
-88
-132
-176
-220
Ziarat
Loralai
ANOMALY FROM MODEL
Fort Munro
D.G. Khan
BOUGUER ANOMALY
KM
-0
10
20
30
40
50
TOPOGRAPHY
ROOF SED. (-0.25)
(-0.1)
(-0.15)
(0.0)
MOLASSE (-0.7)
PRE-COLLISIONAL SED. (-0.15)
(0.0)
TRANSITIONAL CRUST (0)
MANTLE (0.4)
0
100
200
300
400
500
V.E. = 4.00
KILOMETERS

Figure 7c

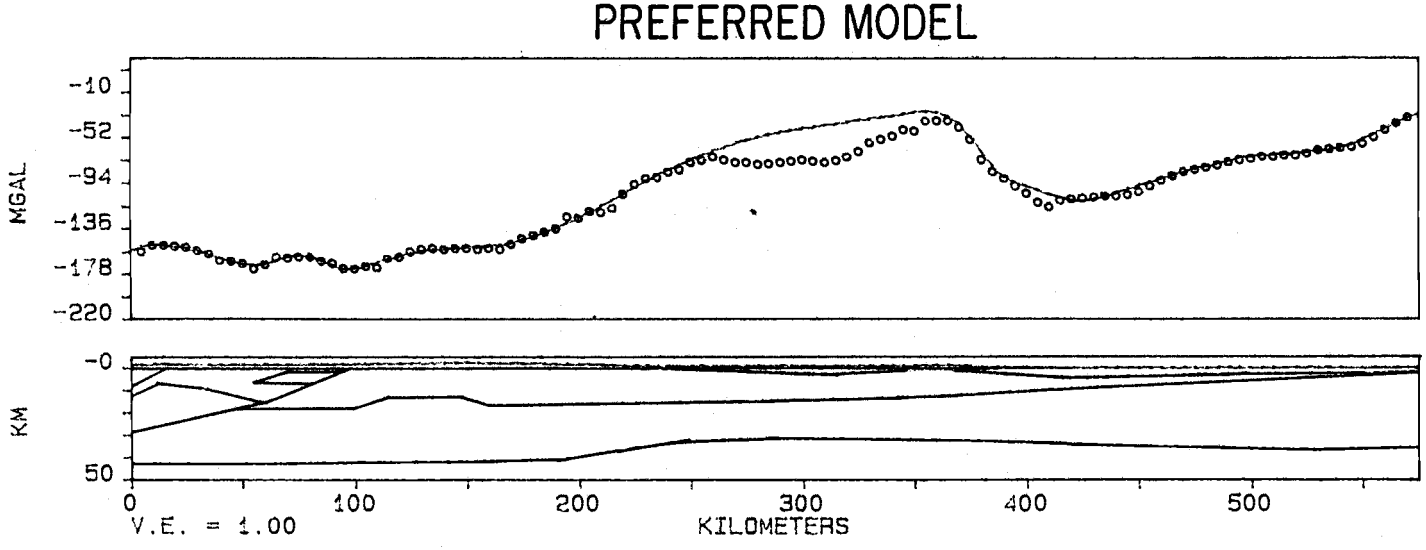
PREFERRED MODEL
MGAL
-10
-52
-94
-136
-178
-220
KM
-0
50
0
100
200
300
400
500
V.E. = 1.00
KILOMETERS

Figure 7d

DISCUSSION OF MODELS

The constructed model in fig. 7 suggests the presence of a 15 to 25 km thick transitional crust underneath the Sulaiman foldbelt, with the gradual shallowing of the Moho from 35 km depth at the 530 km point to about 30 km depth at the 300 km point to the west. Large discrepancy in the observed and the calculated values between the 350 km and 250 km points is in the region where gravity values could not be observed in the field (see map, Map pocket A). Hence, the values in this region were approximated between the values observed along the roads and the nearby gravity contours.

In the central part of the model, the Moho descends steeply between the 270 and 170 km points to about 43 km depth and then flattens out to the west in the Chaman transform fault region. This configuration suggests local isostatic equilibrium in the region (e.g., Warner, 1987), which is also evident from near zero free-air and Airy isostatic gravity values (fig. 4, Table 2).

The calculated gravity in figure 7a depicts the contribution of the low density sedimentary section, relative to the upper part of the crystalline crust. The calculated gravity closely matches with the observed Bouguer gravity from the eastern extremity to about the 350 km point, the Fort Munro gravity high, where observed values are higher than those calculated. One can match the calculated sediments anomaly with the observed Bouguer gravity by decreasing the sediment thickness, but depth to the basement and thicknesses of overlying sediments in the foredeep and at the frontal part of the deformation front are well controlled by seismic reflection and drill hole data (Humayon et al., 1991; Raza et al., 1989). Therefore, little latitude is left to vary these parameters in this area. The calculated anomaly in figure 7b represents the Moho effect, which generally follows the observed Bouguer gravity anomaly towards the west, beyond Fort Munro. However, the calculated Moho effect is much higher than the lower observed Bouguer values in the east, beneath the foredeep.

According to Humayon et al. (1991) basement is encountered at 2 km depth at the Marot well (fig. 2), and dips gently westward at 2.5^{0} on seismic lines. It is 8 km deep near D. G. Khan, more than 12 km near Sakhi Sarwar (fig. 2), and more than 10 km deep near Jandran (Jadoon et al., 1991). Eocene and younger molasse sediments are about 5 km thick at the deformation front and gradually thin out to about 500 meter at Marot in the foredeep area (Humayon et al., 1991). Based on these constraints, some contribution from a deeper level is apparent from the discrepancy between the observed and calculated anomalies in the region between the 500 and 350 km points in figure 7a.

Comparison of figures 7a and 7b reveals that the thick, low-density sediments may be compensated by a slight shallowing of the Moho in the foredeep region. However, farther west in the Loralai region, deepening of the Moho has subdued the effect of the sediment,

and the observed Bouguer gravity curve generally shows the trend of the Moho beyond the Fort Munro anticline, with superimposed effects of short wavelength anomalies. Figure 7c shows the combined contribution of the sediments and upper mantle, which agrees closely with the observed Bouguer gravity.

Transitional or rift-stage crust is suggested through gravity modeling to underlie the Sulaiman region. A 4 to 5 km high and 50 km wide basement high has been interpreted between the 170 km and 120 km points (near Ziarat), which might have developed during the rifting of Gondwanaland, or during later compressional tectonics. It possibly is involved, along with an overlying duplex structure, in lifting of the older sequence to more than 8 km above its regional level (Banks and Warburton, 1986; Humayon et al., 1991; Jadoon et al., 1991). Farther west, beyond the 80 km point, ophiolite bodies are drawn arbitrarily to match the remaining two short wavelength anomalies; Eocene-Oligocene ophiolites and flysch, thrust over the older sediments, are documented by field mapping in that area (Abbas and Ahmad, 1979; Gansser, 1980; Lawrence et al., 1981).

Although no evidences are available to substantiate the existence of the Ziarat basement high, it is plausible considering the nature of the crust interpreted in the region. Outer marginal basement highs have developed on many rifted continental margins, such as the Gulf of Mexico (Hall et al., 1983), along the southwest African continental margin (Gerrard and Smith, 1983), and in the Carolina Trough region (Hutchinson et al., 1983). Such highs are relatively narrow features (10 to 50 km) and extend roughly parallel to the margin for hundreds of kilometers (Hall et al., 1983). The interpreted high at Ziarat may continue in an arcuate manner along the western Indo-Pakistani margin (fig. 2), thus forming a ramp for the emplacement of ophiolites during the Eocene-Oligocene compressional orogeny (R. D. Lawrence, personnel communication, 1990).

An alternate explanation could be that the arching of the basement occurred during later compressional movement, in a manner analogous to the Benton uplift in the Ouachita mountains (Lillie et al., 1983). Reverse faulting of the crystalline basement might have resulted in the southeastward (or eastward) and vertical movement of a portion of the continental margin as the Ziarat uplift. This reverse fault movement could have been accomplished by the reactivation of old normal faults developed during Mesozoic rifting, like in the Zagros region (Jackson, 1980). Some basement lineaments are observed on Landsat imagery in the region by Kazmi (1979), which may possibly be related to the Ziarat high.

Figure 5 shows the roots necessary for the region to attain simple Airy isostatic equilibrium according to the assumptions made. In contrast, the preferred model in figure 7 depicts transitional crust underneath the Sulaiman region. The transitional crust region is wide and varies from 15 to 25 km in thickness, as along many passive margins. For example rift-stage crust of thickness ranging from 7 to 28 km has been observed along the Atlantic

margin of North America (Grow, 1980; Hutchinson et al., 1983). So the presence of crust less than continental thickness (15 to 25 km) under the wide Sulaiman sub-basin, filled with deep marine to shallow marine sediments (Raza et al., 1989), may suggest continuation of the some rift-stage crust adjacent to the west coast of India (fig. 1).

Two levels of deformation can be associated with figure 7 model. On the east, beyond the 200 km point, deformation within sediments appears to be thin skinned as the basement surface appears to be underthrusting in an undeformed state. The broad width and narrow cross-sectional taper of the thrust belt suggest the presence of a weak decollement zone within or at the base of the sedimentary section. The zone could be evaporites as in the Salt Range/Potwar Plateau region (Seeber and Armbruster, 1979; Jaume and Lillie, 1988), or ductile flow within such a thick sedimentary section. At a deep level thick-skinned deformation occurs within the interior of the fold belt, forming the Ziarat basement high and other structures farther west.

PREFERRED MODEL AND ITS TECTONIC IMPLICATION

Gravity modeling suggests the existence of transitional crust underneath the Sulaiman foldbelt. This crust would have been part of Gondwana prior to its breakup, during late Paleozoic to early Mesozoic time. Figures 8 and 9 represent two possible evolutionary models of the tectonic development of the Sulaiman region. The models are the same except that figure 8 represents an Atlantic type passive continental margin, with a pre-existing basement high inherited from Mesozoic rifting. Figure 9 suggests that the basement high developed entirely during later convergence of an Atlantic margin of an even taper. Although both concepts are equally plausible, figure 9 is preferred for the following reasons. (1) The predominance of deep water sediments favors the existence of an open basin. (2) Isostatic assumption in figures 8a and 8b requires thick crust underneath the high, which apparently is equal in thickness to what is calculated in the figure 7 model. During convergence, thickening of the basement may lead to the presence of crust much thicker than that calculated in the figure 7 model, because of the buoyancy of the continental material (McKenzie, 1969). Therefore, the mechanism of crustal thickening discussed above appears to be more consistent with the model shown in figure 9.

The breaking of the Indo-Pakistani block away from the Gondwana Supercontinent is documented by an early Permian unconformity (Raza et al., 1989; Humayon et al., 1991). This unconfirmity probably marks a period of erosion associated with thermal and tectonic uplift during the rifting stage of the craton (e.g., Falvey, 1974). Subsequent tectonic processes, such as subsidence caused by thermal cooling of the lithosphere and sediment loading of thin extended basement, led to the development of the thick wedge of Mesozoic sediments along the western passive margin of the Indo-Pakistani subcontinent. The westward tilt of the craton during the Mesozoic is marked on seismic reflection lines by thickening of the west-dipping Mesozoic sequence in the Sulaiman foredeep area (Raza et al., 1989; Humayon et al., 1991). Passive margin structures are identified along the western shore of India (Naini and Talwani, 1983), and continue onland along the western margin of the Indo-Pakistani subcontinent (fig. 1; Biswas, 1982; Quadri and Shuaib, 1986; Malik et al., 1988). Sea floor spreading and synrift sedimentation continued during the rapid northward journey of the Indo-Pakistani plate during Mesozoic and early Tertiary times (Powell, 1979).

The main Himalayan orogeny began during the middle Eocene and was initiated by head-on collision along the northern margin of the Indo-Pakistani plate (Powell, 1979). However, the northwestern margin collided with the Afghan Block in an oblique fashion during Eocene-Oligocene to Recent (Lawrence et al., 1981). Figure 9b depicts the continents on the verge of convergence during Cretaceous time. The model shows the emplacement of the ophiolite, to the west, marking the closure of the ocean and subsequent deposition of

Figure 8. Schematic diagram suggesting one of the possible models of tectonic evolution of the Sulaiman foreland fold-and-thrust belt. The diagram is based on the gravity model shown in figure 7c.

(a) Atlantic type passive continental margin with an outer basement high inherited from Mesozoic rifting.

(b) Indo-Pakistani western margin loaded with Mesozoic shelf sediments. The margin is subsided under sediment load and due to thermal cooling to attain isostatic equilibrium. Compensation is assumed to occur at 50 km depth.

(c) Present configuration as a result of compressional tectonics since Eocene-Oligocene time. Note subsidence of the basement due to thrusting and increasing sediment load. Shallow Moho beneath the Sulaiman Range may primarily be inherited from earlier passive margin. The model shows crystalline basement involved in later thrusting. Presence of a pre-existing thick crust underneath the high appears to cause space problems during convergence, since shortening may lead to thickening of the crust by more than that suggested by gravity modeling.

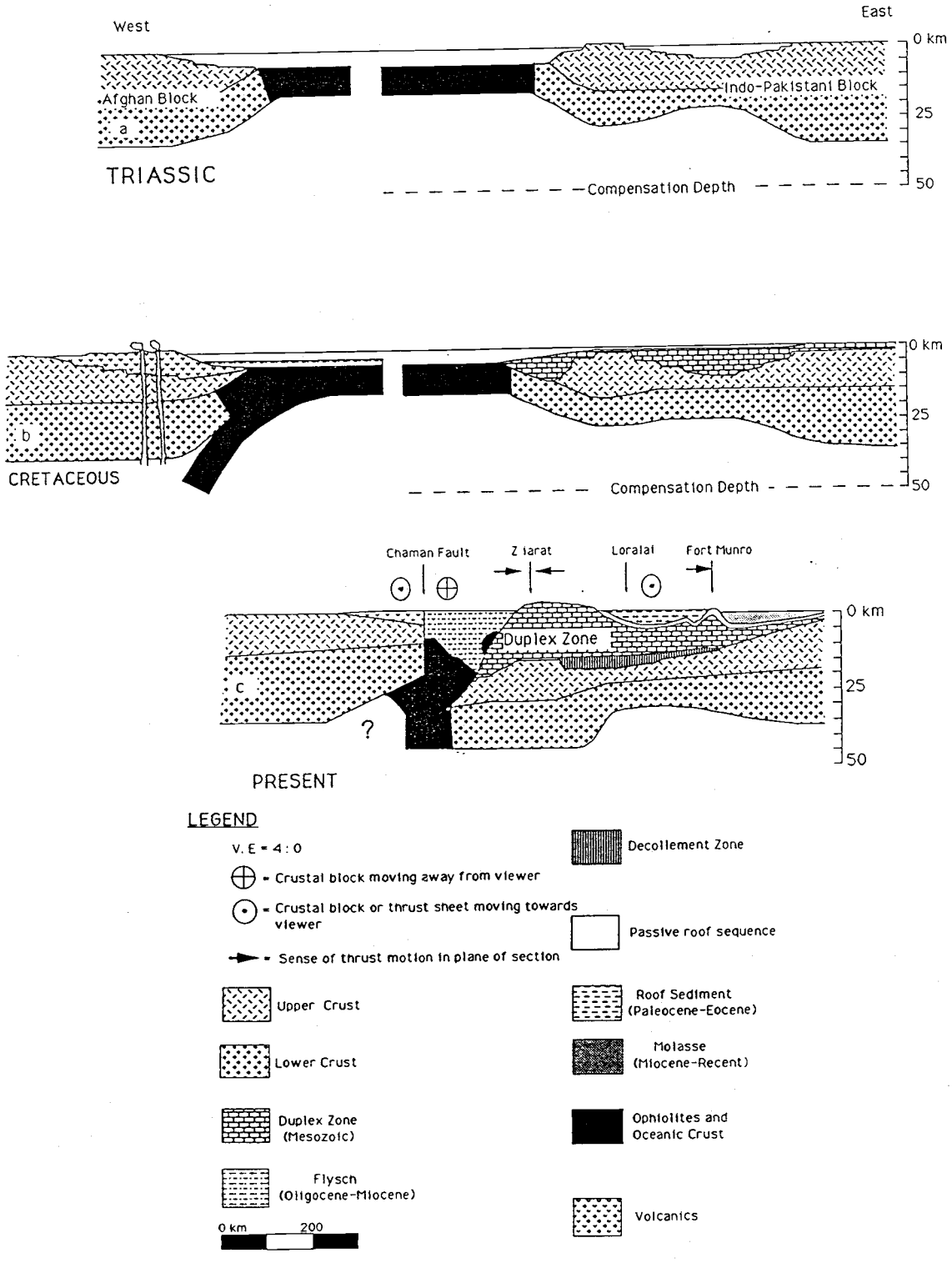
West
East
0 km
Afghan Block
a
Indo-Pakistani Block
25
TRIASSIC
Compensation Depth
50
b
CRETACEOUS
Compensation Depth
Chaman Fault
Z iarat
Loralai
Fort Munro
Duplex Zone
c
?
PRESENT
LEGEND
V. E = 4 : 0
= Crustal block moving away from viewer
= Crustal block or thrust sheet moving towards viewer
= Sense of thrust motion in plane of section
Upper Crust
Lower Crust
Duplex Zone (Mesozoic)
Flysch (Oligocene-Miocene)
0 km
200
Decollement Zone
Passive roof sequence
Roof Sediment (Paleocene-Eocene)
Molasse (Miocene-Recent)
Ophiolites and Oceanic Crust
Volcanics

FIGURE 8

Figure 9. Schematic diagram suggesting alternative tectonic model of the Sulaiman foreland fold-and-thrust belt. The diagram is based on gravity model shown in figure 7c.

(a) Atlantic type passive continental margin inherited from Mesozoic rifting with no outer basement high.

(b) Indo-Pakistani western margin loaded with Mesozoic shelf sediments.

(c) Present configuration as a result of compressional tectonics since Eocene-Oligocene time. Note subsidence of the basement due to thrusting and increasing sediment load. Shallow Moho beneath the Sulaiman Range may primarily be inherited from earlier passive margin. However, some upwarp may be occurring due to underthrusting of Indo-Pakistan crust beneath crust of the Afghan Block. The model shows crystalline basement involved in thrusting, resulting in formation of the Ziarat High. Shortening of the basement is occurring by reverse motion along old basement normal faults (e.g. Jackson, 1980).

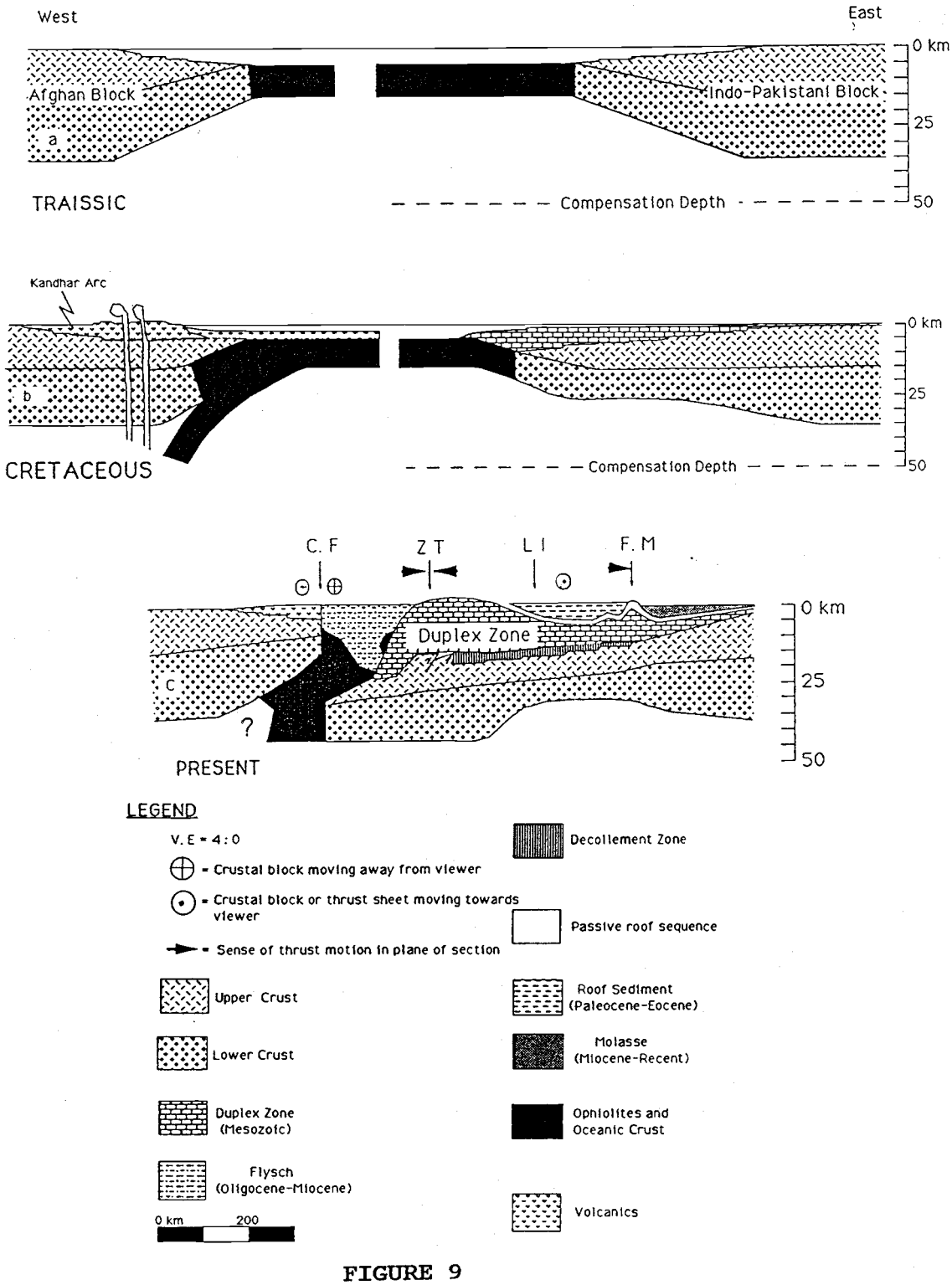
West
East
Afghan Block
Indo-Pakistani Block
a
TRAISSIC
Compensation Depth
0 km
25
50
Kandhar Arc
b
CRETACEOUS
Compensation Depth
C. F
Z T
L I
F. M
Duplex Zone
c
?
PRESENT
LEGEND
V. E = 4 : 0
= Crustal block moving away from viewer
= Crustal block or thrust sheet moving towards viewer
= Sense of thrust motion in plane of section
Upper Crust
Lower Crust
Duplex Zone (Mesozoic)
Flysch (Oligocene-Miocene)
0 km
200
Decollement Zone
Passive roof sequence
Roof Sediment (Paleocene-Eocene)
Molasse (Miocene-Recent)
Ophiolites and Oceanic Crust
Volcanics

FIGURE 9

flysch. The Indo-Pakistani western margin is subsided and loaded with undeformed sediments prior to convergence. Convergence of the Indo-Pakistani plate along its western margin is responsible for the development of the Sulaiman foldbelt, and enormous thickening of the sediments (Banks and Warburton, 1986).

At some stage during convergence, some old normal faults developed during Mesozoic rifting might have absorbed shortening of the basement by reversing their sense of motion. This might have led to the simultaneous development of the Ziarat basement high, crustal thickening, foreland thrusting and thickening of the shelf sediments, and emplacement of flysch and ophiolites. Thrust sheet loading and synorogenic sediment deposition led to the development of the Sulaiman foredeep, like the Ganges foredeep in northern India (Lyon-Caen and Molnar, 1983, 1985), and the Jhelum basin in northern Pakistan (Duroy et al,. 1989). However, unlike the Himalayan foreland, which is underlain by full-thickness continental crust, the thick sedimentary section in the Sulaiman Range is compensated by shallow mantle material, inherited from the Mesozoic rifted margin. A similar gravity model has been presented for the Ouachita Mountains of western Arkanas (Lillie et al., 1983), where the thick sedimentary sequence is also accompanied by shallowing of the Moho.

To the east of Ziarat, the deformation style appears to be thin skinned, as is evident from low topography, broad structures (Jaume, 1986), and the presence of Eocene to Recent sediments (Humayon et al., 1991). It is possible that thick sediments at depth are behaving ductilely (Davis and Lillie, manuscript in preparation), as a result of high temperatures (Raza et al., 1989). At the deformation front, the Fort Munro anticline has probably developed as a result of thrusting of the sediments, either along a basement buttress or along a ramp formed within the sediments due to termination of the weak decollement at shallower depths (Humayon et al., 1991).

Figure 9c shows the tectonic state of the region discussed above and based on the gravity model constructed in figure 7. It represents the combined products of Mesozoic rifting, Eocene to present convergence, and sediment deposition depicted in figures 9a and 9b. Note that the present configuration incorporates a shallowing of the Moho from the earlier passive margin and thickening of the transitional/oceanic crust to the west.

CONCLUSIONS

The gravity model shown in figure 7 combines shallow structures determined from seismic and drill hole data in the foredeep region (Humayon et al., 1991) with geological and structural studies in the hinterland region of the Sulaiman area (Banks and Warburton, 1986; Humayon et al., 1991). Based on the above discussions, conclusions drawn from the gravity observations (figure 4) and the model are:

1) The entire Sulaiman foreland fold and thrust belt is underlain by transitional crust. The crust is wide and relatively thick, like that of the Baltimore Canyon (Grow, 1980) and Carolina Trough region (Hutchinson et al., 1983). The thickness of the crystalline crust, beneath the thick sediments, ranges from 15 to 25 km.

2) Two levels of deformation are identified. One is within the crust, which is deforming under the influence of horizontal compressive forces and the overlying thrust load. The second level of deformation is within the thick overlying sediments, but the exact level (or levels) is not known.

3) The foreland fold-and-thrust belt deviates significantly from ideal Airy isostatic equilibrium. The Fort Munro-Loralai topography lacks crustal roots due to the shallowing of the Moho related to the earlier rifted margin, while the Ziarat topography does have roots and is in local isostatic equilibrium including the region west of it.

4) Interpretation of a passive margin underneath the eastern Sulaiman foldbelt and the presence of ophiolites and Khojak Flysch to the west suggest that the margin is in the initial stages of convergence.

REFERENCES CITED

Abbas, G., and Ahmad, Z., The Muslimbagh ophiolites, in A. Farah and K.A. DeJong, eds., Geodynamics of Pakistan: Geological Survey of Pakistan, Quetta, p.243-250, 1979.

Abdel Gawad, Wrench movements in Baluchistan arc and their relation to Himalayan Indian Ocean tectonics, Geol. Soc. Amer. Bull., v. 82, 1971.

AMOCO Inc., Bouguer gravity map (unpub), sheet 2 of 2; AMOCO Pakistan exploration company, Karachi, Pakistan, 1972.

Banks, C. J., and Warburton, J., Passive-roof duplex geometry in the frontal structures of the Kirthar and Sulaiman mountain belts, Pakistan, J. Struct. Geol., No. 8, p. 229-237, 1986.

Biswas, S.K., Rift basins in western margin of India and their hydrocarbon prospects with special reference to Kutch basin: Bull. Amer. Assoc. Petrol. Geol., p. 1497-1513, 1982.

Chaudary, L. R., Reversal of basement-block motions in Cambay basin, India and its importance in Petroleum exploration, AAPG. Bull., v. 59, p. 84-96, 1975.

Chun, K.Y., Crustal block of the western Ganga basin: A fragment of oceanic affinity ?, Seis. Soc. Amer. Bull., v. 76, No. 6, p. 1687-1698, 1986.

Davis, D. M., and Lillie R. J., Changing Mechanical Response During Continental Collision: Active Examples from the Foreland Thrust Belts of Pakistan. Manuscripts in prepration, 1991.

Dobrin, M. B., and Savit, C. H., Introduction to geophysical prospecting, fourth edition, McGraw-Hill Book Company, Inc., 1988.

Duroy, Y., Farah, A., and Lillie R. J., Subsurface densities and lithospheric flexure of the Himalayan foreland in Pakistan, in Tectonics of the Western Himalayas, edited by L. L. Malinconico and R.J. Lillie, Geol. Soc. Amer., Spec. papar 232, p. 217-236, 1989.

Falvey, D. A., The development of continental margins in plate Tectonic theory: Aust. Pet. Expl. Asso. J., v. 14, p. 95-106, 1974.

Farah, A., and Zaigham, Gravity anomalies of the ophiolite complex of Khanozai-Muslimbagh-Nasai-Qila Saifullah area, Zhob district, Baluchistan, in Geodynamics of Pakistan, edited by A. Farah and K. A. DeJong, Geol. Surv. Pakistan, Quetta, p. 251-262, 1979.

Farah, A., Lawwrence, R. D., and DeJong, K. A., An overview of the tectonics of Pakistan, in Marine Geology and Oceanography of Arabian Sea and Coastal Pakistan, eds, B. U. Haq and J.D. Milliman, Van Nostrand Reinhold, p. 161-176, 1984.

Gansser, A., The Peri-Indian suture zone, Geologie de chaines Alpines issues de La Tethys, colloque, c 5, 26th Int. geol. cong., 1980.

Gerrard, I., and Smith, G. C., Post-Paleozoic succession and structure of the Southwestern African continental margin, in J. S. Watkins and C. L. Drake, eds., Studies in continental margin geology: AAPG Memoir 34, p. 49-76, 1983.

Grow, J. A., Deep structure and evolution of the Baltimore Canyon trough in the vicinity of the COST No. B-3 well, in P. A. Scholle, ed., Geological studies of the COST No. B-3 well, United States Mid-Atlantic continental slope area: U. S. Geological Survey Circular 933, p. 117-125, 1980.

Hall, D. J., Cavanaugh, T. D., Watkins, J. S., and McMillen, K. J., The rotational origin of the Gulf of Mexico based on regional gravity data, in J. S. Watkins and C. L. Drake, eds., Studies in continental margin geology: AAPG Memoir 34, p. 115-128, 1983.

Heiskanen, W. A., and Meinesz, F. A. V., The earth and its gravity field, McGraw-Hill series in the geological sciences; McGraw-Hill Book Company, Inc. 1958.

Hemphill, W. R., and Kidwai, A. H., Stratigraphy of the Bannu and Dera Ismail Khan areas, Pakistan: U. S. Geol. Surv. Professional Paper, 716 B, 36p, 1973.

Humayon, M., Lillie R. J., and Lawrence R. D., Structural interpretation of the eastern Sulaiman foldbelt and foredeep, Tectonics, in press, 1991.

Hutchinson, D. R., Grow, J. A., Klitgord, K. D., and Swift, B. A., Deep structure and evolution of the Caroliina Trough, in J. S. Watkins and C. L. Darke, eds., studies in continental margin geology, AAPG Memoir 34, p. 129-152, 1983.

Jackson, J. A., Reactivation of basement faults and crustal shortening in orogenic belts, Nature, v. 283, p. 343-346, 1980.

Jadoon, I. A. K., Lawrence R. D., and Lillie R. J., Balanced and retrodeformed geological cross-section from the frontal Sulaiman lobe, Pakistan: Duplex development in thick strata along the western margin of the Indian plate, in Thrust Tectonics, edited by K. McClay, in press, Publisher Unwin Hyman, 1991.

Jaume, S. C., The mechanics of the Salt Range-Potwar Plateau, Pakistan: quantitative and qualitative aspects of a fold-and-thrust belt underlain by evaporites, M. S. thesis, Oregon State University, Corvallis, Oregon, 58 p., 1986.

Jaume, S. C., and Lillie, R. J., Mechanics of Salt Range/Potwar Plateau, Pakistan: A Fold-and thrust belt underlain by evaporites, Tectonics, 7, p. 57-71, 1988.

Jones, A. G., ed., Reconnaissance Geology of part of West Pakistan, ed., A Colombo Plan Cooperative project: Hunting Survey Corporation, Maracle Press, Toronto, Ontario, 550 p., 1961.

Kaila, K. L., Structure and seismotectonics of the Himalaya-Pamir-Hindukush Region and the Indian plate bouundary, in Zagros-Hindukush-Himalaya Geodynamic Evolution, H. K. Gupta and F. M. Delany, eds., AGU., Washington, D. C., Geol. Soc. Amer., Boulder, Colorado, p. 272-293, 1981.

Karner, G. D., and Watts, A. B., Gravity anomalies and flexure of the lithosphere at mountain ranges: J. Geoph. Res., 88, 10449-10477, 1983.

Kazmi, A. H., Active fault system in Pakistan, in A. Farah and K. A. DeJong, eds., Geodynamics of Pakistan, Geol. Surv. Pakistan, Quetta, Pakistan, p. 285-294, 1979.

Kazami, A. H., and Rana R. A., Tectonic Map of Pakistan, scale 1:2,000, 000, Geol. Surv. Pakistan, Quetta, Pakistan, 1982.

Lawrence, R. D., and Yeats, R. S., Geological reconnaissance of the Chaman fault in Pakistan, in A. Farah and K. A. DeJong, eds., Geodynamics of Pakistan, Geol. Surv. Pakistan, Quetta, Pakistan, p. 351-357, 1979.

Lawrence, R. D., Khan S. H., DeJong K. A., Farah A., and Yeats R. S., Thrust and strike slip fault interaction along the Chaman transform zone, Pakistan, Geol. Soc. London, Spec. Pub. 9, p. 363-370, 1981.

Lawrence, R. D., and Khan S. H., Structural reconnaissance of Khojak Flysch, Pakistan and Afghanistn, Tectonics, in review, 1990.

Lillie, R. J., Nelson, K. D., DeVoogd, B., Brewer, J. A., Oliver, J., E., Brown, L. D., Kaufman, s., and Viele, G. W., Crustal structure of the Ouachita Mountains, Arkansas: A model based on integration of COCORP reflection profiles and regional geophysical data, Amer. Assoc. Pet. Geol. Bull., 67, p. 907-931, 1983.

Lillie, R. J., Johnson, G. D., Yousaf, M., Zamin, A. S. H., and Yeats, R. S., Structural development within the Himalayan foreland fold-and-thrust belt of Pakistan, in sedimentary basins and basin forming mechanisms, eds., C. Beaumont and A. J. Tankard, Canadian Soc. Petrol. Geol., Memoir 12, p. 379-392, 1987.

Lyon-Caen, H., and Molnar, P., Constraints on the structure of the Himalaya from an analysuis of gravity anomalies and a flexure model of the lithosphere, J. Geoph. Res., 88, p. 8171-8191, 1983.

Lyon-Caen, H., and Molnar, P., Gravity anomalies, flexure of the Indian plate, and the structure, support and evolution of the Himalaya and Ganges Basin, Tectonics, 4, p. 513-538, 1985.

Malik, Z., Kemal, A., Malik, A., and Bodenhausen, J. W., Petroleum potential and prospects in Pakistan: International Symposium on Petroleum for the Future, Jan. 28-30, Islamabad, Ministry of Petroleum and Natural Resources, Pakistan, 1988.

Malinconlco, L. L. Jr., The structure of the Kohistan-Arc in Northern Pakistan as inferred from Gravity Data, Tectonophysics, 124, p. 297-307, 1986.

Malinconico, L. L. Jr., Crustal thickness estimates for the western Himalaya, in Tectonics of the western Himalyas, edited by L. L. Malinconico, Jr., and R. J. Lillie, Geol. Soc. Amer., Spec. Paper 232, p. 237-242, 1989.

Marussi, A., Geophysics of the Karakorum. "Ital. Exped. to the Karakorum (K^2) and Hindu-Kush, A. Desio, leader", Scient. Reports, II, v. 1, Brill, Leiden, 1964.

Marussi, A., Introductory report of Geophysics, in Geotettonica Delle Zone Orogeniche Del Kashmir Himalaya, Karakoram-Hindu Kush-Pamir, Accademia Nationale dei Lincei, 21m 15-25, 1976.

Marussi, A., Gravity, crustal tectonics and mantle strructure in the Central Asian Syntaxis, Proc. Intern. Commit. Geodynamics, Grp. 6, Mtg. Peshawar, Nov. 23-29, 1979: Spec. Issue, Geol. Bull. Univ. Peshawar, Vol. 13, 1980.

McGinnis, L. D., Gravity field and tectonics in the Hindu-Kush, J. Geoph. Res., 76, 1894-1904, 1971.

McKenzie, D. P., Speculation on the consequences and causes of plate motion, Geophy. J. Roy. Astro. Soc., 18, p. 1-32, 1969.

Menki, W. H., and Jacob, K. H., Seismicity patterns in Pakistan and northwestern India associated with continental collision, Seis. Soc. Amer. Bull., v. 66, No. 5, p. 1695-1711, 1976.

Molnar, P., and Tapponnier, P., Cenozoic tectonics of Asia: effects of a continental collision, Science, 189, p. 419-426, 1975.

Molnar, P., and Tapponnier, P., Active tectonics of Tibet, JGR., 83, p. 5361-5375, 1978.

Nafe, J. E., and Dark, C. L., Society of Exploration Geophysicists, Annual Meeting, 1957, Unpublished paper. The graph referred to is published in R. E. Sheriff, Encylopedic Dictionary of exploration Geophysics, Society of Exploration Geophysicists, 2nd Ed., p. 164, 1984.

Naini, B. R., and Talwani, M., Structural framework and evolutionary history of the continental margin of western India: in J. S. Watkins, and C. L. Drake, eds., Studies in continental margin geology: AAPG. Mem. 34, p. 167-192, 1983.

Powell, C. M., A Speculative tectonic history of Pakistan and surroundings: Some constraints from the Indian ocean: in A. Farah and K. A. DeJong, eds., Geodynamics of Pakistan, Geol. Surv. Pakistan, Quetta, Pakistan, p. 5-24, 1979.

Quadri, V. N., and Shuaib, M., Hydrocarbon prospects of southern Indus basin, Pakistan: AAPG. Bull., v. 70, p. 730-747, 1986.

Quittmeyer, R. C., Farah, A., and Jacob, K. H., The seismicity of Pakistan and its relation to surface faults: in A. Farah and K. A. DeJong, eds., Geodynamics of Pakistan, Geol. Surv. Pakistan, Quetta, Pakistan, p. 351-358, 1979.

Rabinowitz, P. D., and Labrecque, J. L., The isostatic gravity anomaly: Key to the evolution of the ocean-continent boundary at passive conttinental margins, Earth and Planetary Science Letters, 35, p. 145-150, 1977.

Rahman, A., Crustal section across the Sibi-Syntexial-Bend, West Pakistan, based on gravity measurements, J. Geoph. Res., 74, p. 4367-4370, 1969.

Raza, H. A., Ahmed, R., Ali, M. S.,and Ahmad, J., Petroleum prospects: Sulaiman sub-basin, Pakistan; Pakistan Journal of Hydrocarbon Research, Hydrocarbon Develop. Inst. Islamabad, Pakistan, v. 2, 21-56, 1989.

Rowlands, D., The structure and seismicity of a portion of the southern Sulaiman Range, Pakistan, Tectonophysics, 51, p. 41-56, 1978.

Royden, L., and Karner, G. D., Flexure of Lithosphere Beneath Apennine and Carpathian Foredeep Basin: Evidence for Insufficient Topographic Load, AAPG. Bull., v. 68, No. 6, p. 704-712, 1984.

Sarwar, G., and DeJong K. A., Arcs, oroclines, syntaxis: The curvature of mountain belts in Pakistan, in A. Farah and K. A. DeJong, eds., Geodynamics of Pakistan, Geol. Surv. Pakistan, Quetta, Pakistan, p. 351-358, 1979.

Seeber, L., and Armbruster, J. G., Seismicity of the Hazara arc in northern Pakistan; decollement vs. basement faulting, in A. Farah and K. A. DeJong, eds., Geodynamics of Pakistan, Geol. Surv. of Pakistan, Quetta, Pakistan, p. 131-142, 1979.

Seeber, L., Armbruster, J. G., and Quittmeyer, R. C., Seismicity and continental subduction in the Himalayan arc, H. K. Gupta and F. M. Delany, eds, Zagros, Hindukush, Himalaya Geodynamic evolution, AGU., Geodynamics Series 3, p. 215-242, 1981.

Sengupta, s., Ray, K. K., Acharyya, S. K., and deSmeth, J. B., Nature of ophiolite occurrences along the eastern margin of the Indian plate and their tectonic significance, Geology, v. 18, No. 5, p. 439-442, 1990

Talwani, M., Woezel, J. L., and Landisman, M., Rapid gravity computations for two-dimensional bodies with application to the Mendocino submarine fracture zone, JGR., 64, 49-59, 1959.

Verma, R. K., Bhanja, A. K., and Mukhopadhyay, M., Seismotectonics of the HinduKush and Baluchistan arc,Tectonophysics, 66, p. 301-322, 1980.

Verma, R. K., and Subrahmanyam, C., Gravity anomalies and the Indian lithosphere: review and analysis of existing gravity data, Tetonophysics, 105, p. 141-161, 1984.

Warner, M. R., Seismic reflection from the Moho - the effect of isostasy, Geophy. J. R. Ast. Soc., 88, p. 425-435, 1987.